Kéage Laboratory of Nuclear science Decennial Report 1966-1976

AUTHOR(S):

Yanabu, Takuji

CITATION:

Yanabu, Takuji. Kéage Laboratory of Nuclear science Decennial Report 1966-1976. Bulletin of the Institute for Chemical Research, Kyoto University 1977, 55(1): 74-133

ISSUE DATE:

1977-03-31

URL:

http://hdl.handle.net/2433/76710

Bull. Inst. Chem. Res., Kyoto Univ., Vol. 55, No. 1, 1977

Review

Kéage Laboratory of Nuclear Science Decennial Report 1966-1976

Takuji YANABU*

Received January 10, 1977

The activities of the Kéage Laboratory of Nuclear Science in the period from 1966 to 1976 are summarized and reviewed. This report is a continuation of a report written by K. Kimura in 1965. Layout of the laboratory, development of nuclear instrumentations, researches in nuclear physics and chemistry, are grouped into sections and trends in the history of the laboratory are described.

I. INTRODUCTION

The decenninal report from 1955 to 1965 was written by K. Kimura and published in the Bulletin of the Institute for Chemical Research, Kyoto University, volume 43, p. 499 (1965). In this report, research activities of the Kéage Laboratory of Nuclear Science since the completion of the Kyoto University Cyclotron were compiled and reviewed along with the description of site and building. Since this report was published, one more decade has flowed away over the Laboratory, and we think it necessary to report the history of the laboratory since 1966.

Crudely speaking, the decade from 1955 to 1965 was a period of initiation, and the following decade from 1966 to 1976 was a period of refinement. So far as the organization is concerned, a post of full professorship was established in the nuclear science research facility in 1972 and the late Professor Y. Uemura was appointed as the head of the research facility for the first time. The name Kéage Laboratory of Nuclear Science is only conventional and consists of two branches, that is, Nuclear Science Research Facility and Laboratory of Nuclear Reaction. Unfortunately, Professor Uemura died unexpectedly in 1972, these two laboratories were managed commonly until 1976, when Professor H. Takekoshi was appointed as the head of the Nuclear Science Research Facility. Therefore, from now on, the Nuclear Science Research Facility and the Laboratory of Nuclear Reaction will have partly different and partly common histories. On the other hand, the most important affair in this decade is the improvement of the cyclotron. The cyclotron constructed in 1955 was shut down in 1970 due to the failure of cooling pipes inside the acceleration chamber and remodeled in the period from 1969 to 1973. Other important affairs are; the installation of a mini-computer to use on line data processing and the installation of a beam irradiation and pneumatic transport system. In the following, the history of the Kéage Laboratory in the decade from 1966 to 1976 are summarized into several sections.

* 柳父琢治 : Laboratory of Nuclear Reaction, Institute for Chemical Research, Kyoto University, Kyoto.

II. SITE AND BUILDING

The variations in site and building in this decade are rather small. Topics to be mentioned are as follows. A small pre-fabricated room was constructed in 1972 and has been used as an office of the laboratory of nuclear reaction. Secondly, a water cooling tower was installed in 1969 and the cooling system for the cyclotron and all other equipments in the Facility took a closed form. Until then, city water was used as coolant for oil diffusion pumps and for slit systems of the beam transportation, and moreover, the secondary cooling water of the cyclotron in the water pool was replaced by fresh city water whenever its temperature rose more than 35°C. As a result of the installation of the cooling tower, the expenditure of the cyclotron maintenance decreased by a large amount. Third topic is the re-inforcement of radiation shielding. The shielding between the cyclotron area and the first basement and between the experimental area and the electronic workshop were made by concrete blocks until recently but in 1974, they were replaced by motor driven concrete doors and a permanent concrete maze respectively. As a result of these radiation shielding re-inforcement, the radiation levels outside the cyclotron area and the experimental area decreased by one order and are far below the allowable dose even if the cyclotron is in operation. Fourth topic is the re-freshment of the electric power supply. The old power supply system was endowed from the Kansai Electric Power Co., Inc. in 1953. This system had pursued its role and replaced

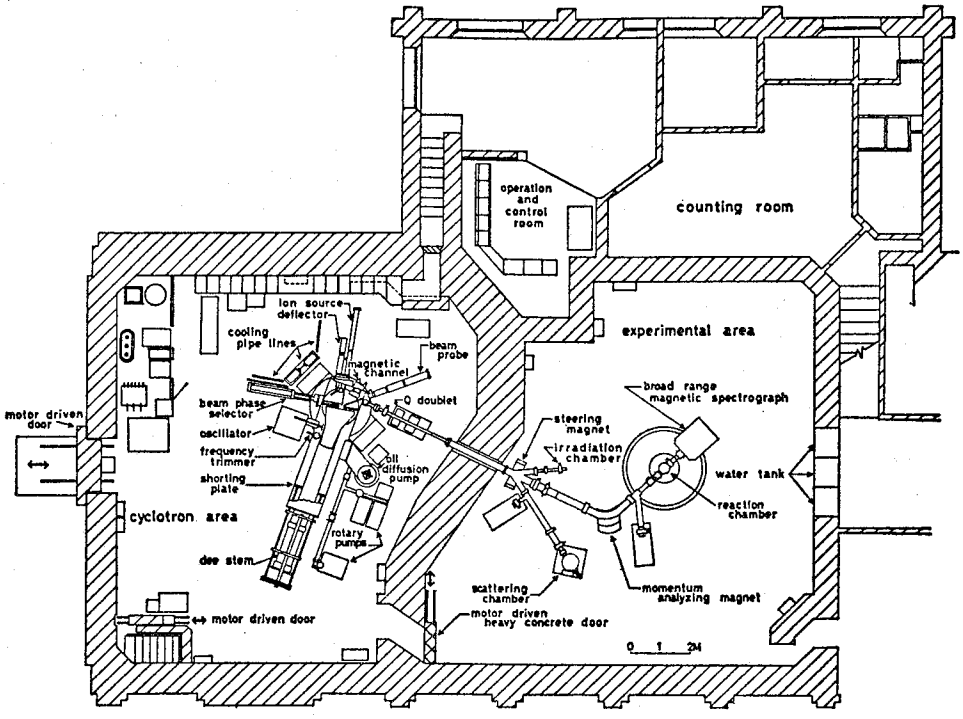

Fig. 2–1. Arrangement of the cyclotron and beam lines in 1975. The right hand side of the building faces to the north. From [74–5].

with new system in 1973. Low voltage wiring inside the research facility was also replaced with new ones in 1975. Present day arrangement of the cyclotron and beam lines are shown in Fig. 2–1.

Other things are almost equal to those in 1965.

III. ACCELERATOR PHYSICS

The most important affair in the history of the laboratory in this decade is the improvement of the cyclotron. Three papers were published about the improvement; [74–4], [74–5], and [74–6]. Since 1965 troubles occurred frequently and in the fall of 1967, it was concluded that the life span of the cyclotron was expired. In March, 1970, the cyclotron was shut down and the renewal works began. The cyclotron and its operation systems were completely remodeled except for the main magnet. In the design study of the remodeling, following principles were adopted.

Table III–1. Differences between the Old and New Cyclotron From [74–5]

Items	Before remodeling (old cyclotron)	After remodeling (new cyclotron)
Main magnet	pole tip 105 cm	no difference
Magnetic field	17.5 kG	15 kG–17.5 kG
Gap between pole tips	135 mm	144 mm
Type of dee	double dees	single dee
Dee voltage	dee to dee 100 kV	dee to ground 100 kV
Position of deflector	inside the dee	outside the dee
Deflector voltage	45 kV	100 kV
Magnetic channel	none	3 rods system
Resonant cavity	double quarter wave lines	single quarter wave line
Dimensions of cavity	inner shell 200 mm	inner shell 400 mm
	outer shell 600 mm	outer shell 1,200 mm
Line termination	shorting condenser	shorting plate
Resonant frequency	13 MHz	11–18 MHz
Type of oscillator	D. C. biased oscillator	booster and main oscillator
Osc. power tube	8T71×2	7T40+9T82
Oscillator out put	75 kW	120 kW
Coupling of osc. to resonant cavity	L-coupling	C-coupling
Main evacuating pump	2,500 *l*/s o.d.p.×2	10,000 *l*/s o.d.p.×1. Oil 4.2 *l*
Booster pump	80 *l*/s o.d.p.	800 *l*/s o.d.p.
Helium leak detector	none	equipped to the main pump
Type of ion source	single arm, hooded arc	dual arm, hooded arc
I. S. arc voltage	300 V single stage	300 V+500 V, two stage
Lithium ion source	none	metal bombarded by electrons
Beam energies	H 7.5 MeV	6–7.5 MeV
	D 15 MeV	12–15 MeV
	He (3)	30–40 MeV
	He (4) 30 MeV	24–30 MeV
	Li (6)	max. 44 MeV

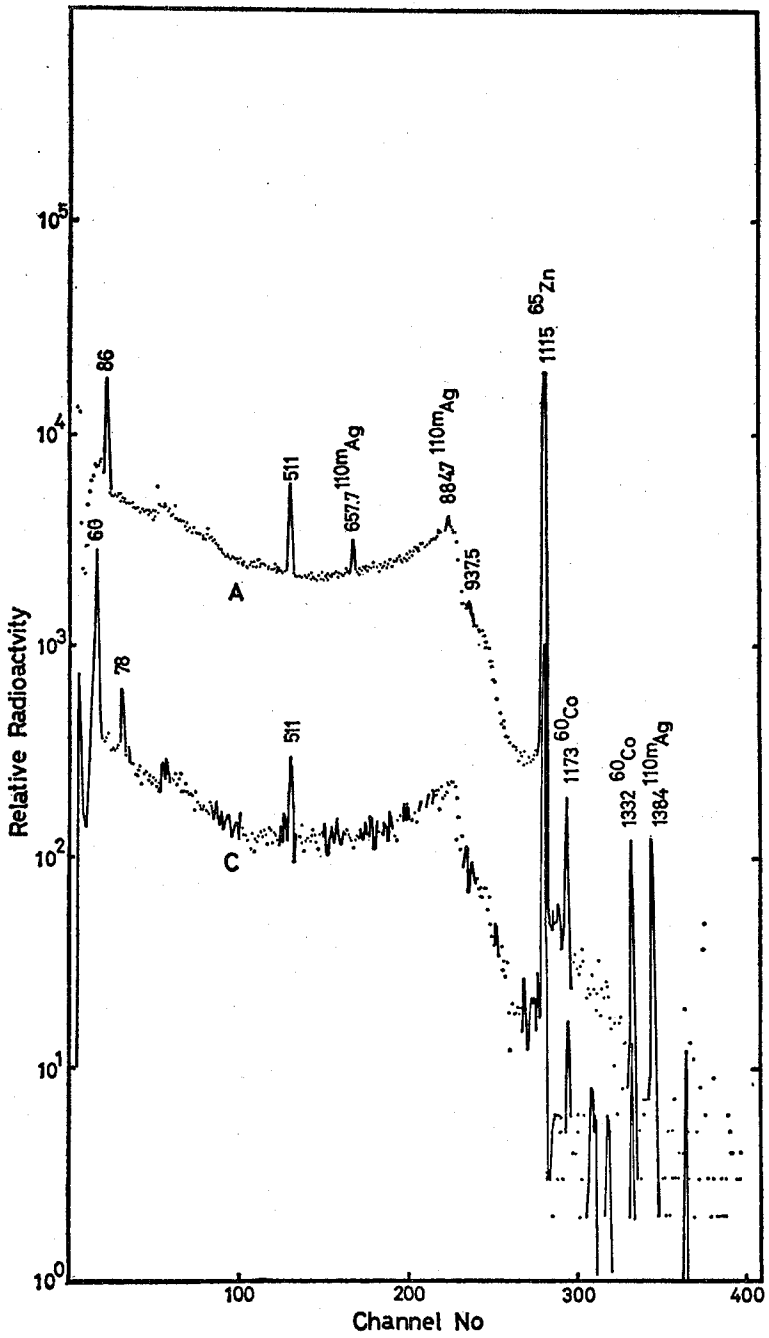

Fig. 3–1. Gamma ray spectra of samples smeared out from the deflector of the old cyclotron. A and C in the figure denote the position of the smearing. See ref. [74–6].

First, the frequency of the R. F. oscillation could be varied as wide as possible to accelerate ^{3}He ions and heavy ions besides the protons, deuterons and alpha particles. This variable frequency made it possible on the other hand to vary the energy of a beam. The paper [74–4] deals with the R. F. characteristics. To vary the frequency, single dee, single coaxial line system was adopted. This system has some difficulties when compared with that of the old cyclotron. One difficultly is how to overcome the multipactoring phenomenon and another problem was how to maintain the frequency as constant as possible. As described in [74–4], multipactoring phenomenon was overcome by adjusting the coupling strength between the resonant cavity and the oscillator. To maintain the frequency constant, feed back systems of the capacity trimming and inductance trimming were designed. Among these two methods, inductance trimming method was preferable and the frequency is now stabilized within 100 Hz at the R. F. range from 11 MHz to 18 MHz. The paper [74–5] deals with the detailed explanation of the design and construction of the cyclotron improvement. Table III–1 gives the differences of characteristics between the old and new cyclotron. In this paper, [74–5], magnetic field shimming, vacuum system, cooling system, acceleration system, control system and the performance of the cyclotron are described. The renewed cyclotron is in operation since 1973. The third paper, [74–6], deals with the residual activity of the old cyclotron. This investigation was done by Prof. Nishi *et al.* of the Research Institute for Atomic Energy. In Fig. 3–1 is shown the gamma ray spectra of samples smeared out from several portions of the deflector of the old cyclotron. The radioactivity of the dust in the acceleration chamber was also estimated. In Table III–2 the results are listed. From these measurements, it is seen that most of the long-lived radioactivities are due to ^{65}Zn. This nuclide is supposed to be produced by reactions such as $^{65}Cu(p,n)$, $^{63}Cu(d,\gamma)$, $^{65}Cu(d,2n)$, and $^{63}Cu(\alpha,2n\beta^{-})$. Therefore, these activities are due to the bombardment of stray beams on the acceleration chamber made of brass.

Table III–2. Relative Radioactivity of the Dust in the Acceleration Chamber. Chemical Separation was Performed. Measurements were made *on from 4th to 6th of Feb. 1971. From [74–6].*

Sample	Relative activity (μC_i)							
	^{22}Na	^{60}Co	^{65}Zn	^{95}Nb	$^{110}Ag^{m}$	^{183}Re	$^{183}Re^{m}$	^{185}Os
Gross dust	1.98(−4)	6.46(−4)	1.43(−1)		1.71(−3)	8.09(−3)	2.21(−3)	
Chemically separated dust								
Cu-group sulfide			4.72(−3)		1.65(−3)	5.01(−3)	1.06(−2)	
Cd-group sulfide			6.68(−3)			1.21(−3)	3.25(−3)	6.55(−4)
Zn fraction			1.58(−1)					
Co fraction		2.23(−3)						
Ta fraction				1.1(−2)*				
R.E. fraction						7.83(−3)	2.39(−2)	
Insoluble			2.71(−2)					

* Activity of Ta fraction was measured on another sample, and is roughly one thousandfold intense relative to the other figures.

Aside from the cyclotron improvement, four papers were published in this decade. Two of them dealt with the electron extraction experiment from the INS electron synchrotron [67–2], [68–7]. These experiments were done in collaboration of University of Tokyo, Institute for Nuclear Study and Institute for Chemical Research, Kyoto University. Two kinds of extraction method were tried and both methods succeeded in the beam extraction. In 1966, the Piccioni's slow extraction scheme was applied to the INS electron synchrotron. In this method, shrinked orbit of the electron beam at the final stage of the acceleration was further disturbed by a set of absorbers made of Be. The perturbed orbit of electrons enters the first kicker magnet and then is deflected outwards. This outgoing electrons are deflected further by the second kicker magnet and extracted from the synchrotron. Extraction efficiency of this method was estimated to be 10% at the electron energy of 540 MeV. Time duration of the extracted beam was 700 μs. Figure 3–2 shows the extraction system by this method. In 1968, another method of slow extraction, one-third resonance method, was applied to the same machine. One-third resonance means that the number of the betatron oscillation per revolution is modified to an integer times 1/3. The ν_r is 2.25 in an ordinary operation. A current strip inserted in the straight section of the synchrotron disturbes the electron orbit and ν_r becomes 7/3. In this case, vertical oscillation resonates with horizontal oscillation and the amplitude of horizontal betatron oscillation becomes very large and the beam enters the kicker magnet. By the aid of first and second kicker magnet, the electron beam is extracted from the synchrotron. Figure 3–3 shows the layout of the extraction system and Fig. 3–4 shows the cross sectional view of the current strip. By this one-third resonance method, the extraction efficiency and time duration of the beam were far more improved than those by the Piccioni's method. In Fig. 3–5, the extraction efficiency is shown as a function of the current of the current strip. The maximum extraction efficiency reaches 50%. The duty cycle of the beam was estimated to be

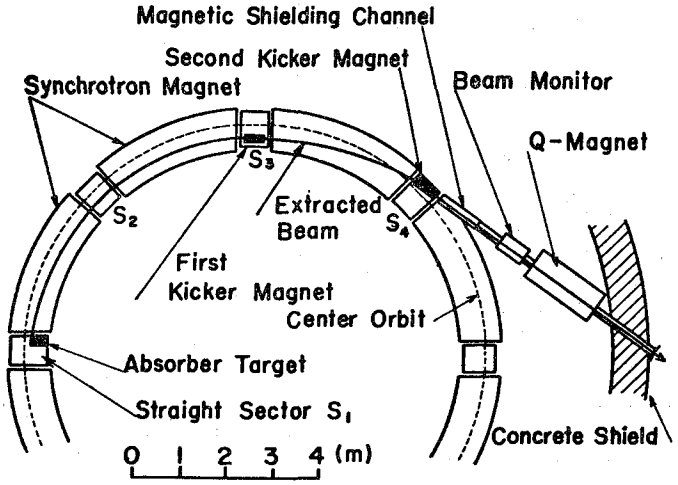

Fig. 3–2. A plan view of the extraction system according to Piccioni's scheme. From [67–2].

3%; this value is very great value in the existing electron synchrotron. Electron beams thus obtained were used in this decade in various investigations such as electroproduction of pions and electron proton quasi-free scattering in the nucleus and so on. For the electron-proton quasi free scattering, a brief explanation is given in section XIV.

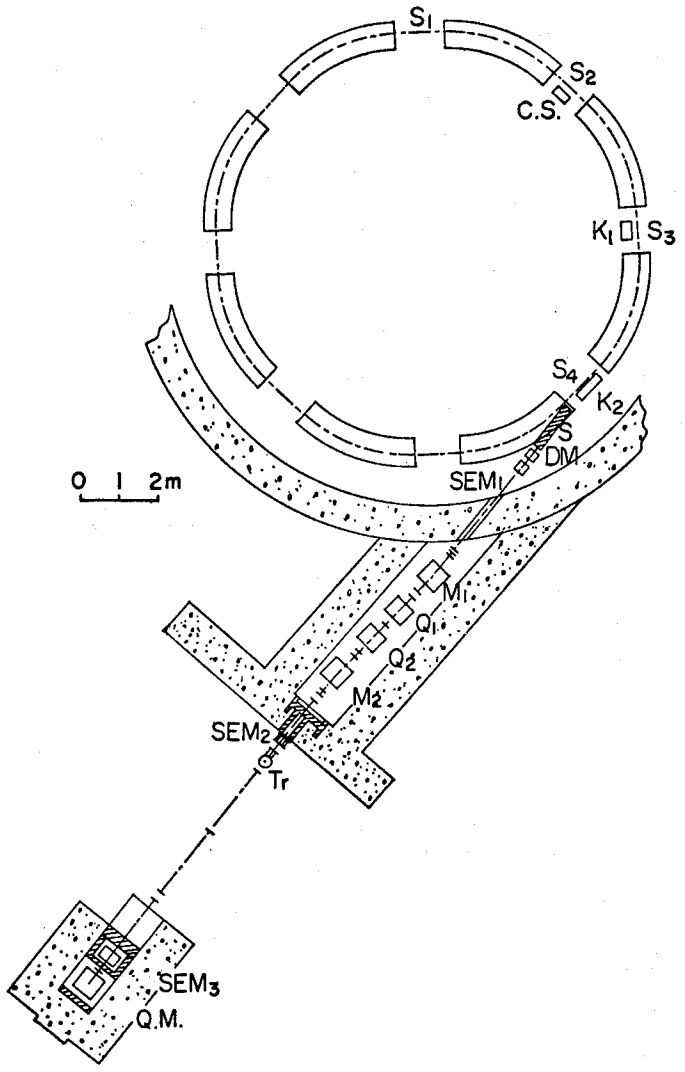

Fig. 3–3. A plan view of the one-third resonance extraction system. C.S.: Current strip. K: Kicker magnet. S: Magnetic shield channel. D.M.: Deflection magnet. SEM: Secondary emission monitor. M: Analyzing magnet. Q: Quadrupole magnet. Tr: Liq. H_2 target. Q.M.: Quantameter. From [68–7].

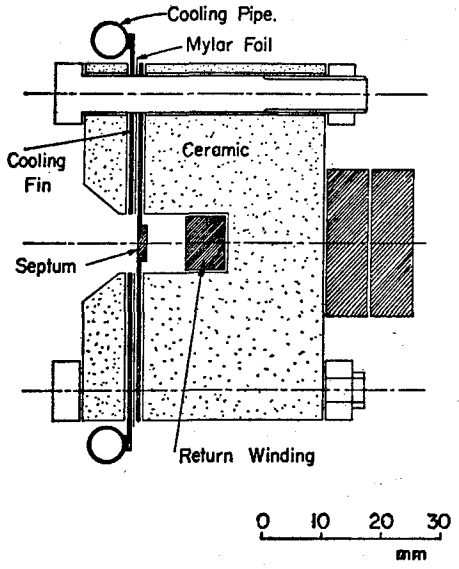

Fig. 3–4. A cross sectional view of the current strip. From [68–7].

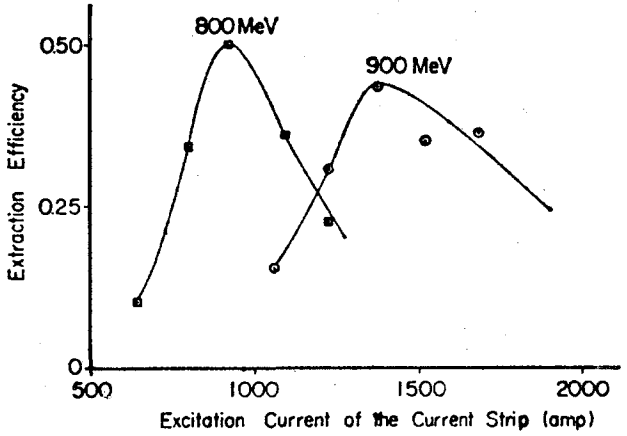

Fig. 3–5. The dependence of the extraction efficiency on the current of the current strip. The position of the septum of the current strip is 30 mm inside from the center orbit. From [68–7].

On the last, we mention the investigations about the ion source of the cyclotron [69–7]. This paper describes the experiences and improvements during 1957 through 1970 when the cyclotron was shut down. The late Professor Uemura was the leader of this investigation. Trial and cut was repeated and better materials were searched one after another and final form was attained as shown in Fig. 3–6. Leak valve for gas inlet was also developed and the reproducibility and fine adjustment of the gas

supply was established. Figure 3–7 shows the structure of the needle valve thus developed. By the use of this sophisticated ion source system, deflected beam current of 90 μA of H_2^+ ions and 28 μA of He^{2+} ions were obtained. Figure 3–8 shows the deflected beam intensity as functions of arc current. The cyclotron in our laboratory

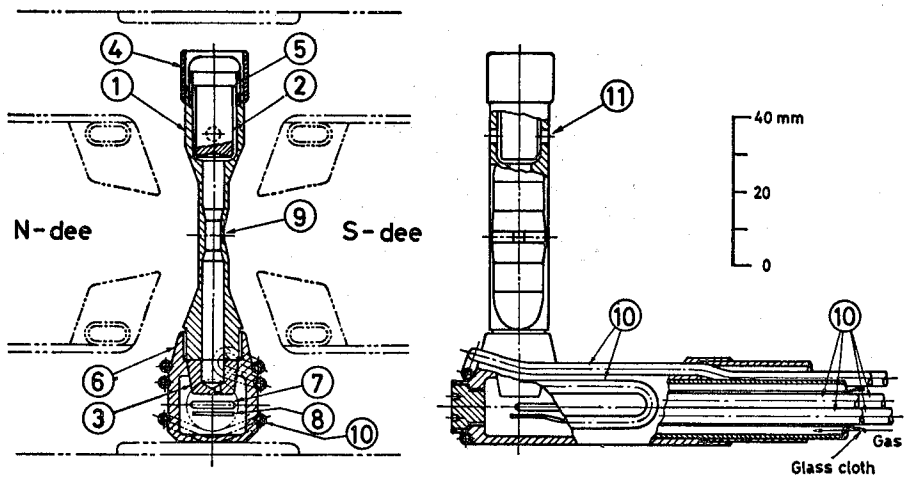

Fig. 3–6. Structure of ion source. 1. Cavity body (Mo). 2. Repeller (W). 3. Canal electrode (W). 4. Shielding tube (Mo). 5. Insulating tube (Quartz). 6. Filament chamber (Cu). 7. Filament (W). 8. Protector plate (W). 9. Aperture for ion extraction. 10. Water-cooling pipe (Cu). 11. Hole for lowering gas pressure. From [69–7].

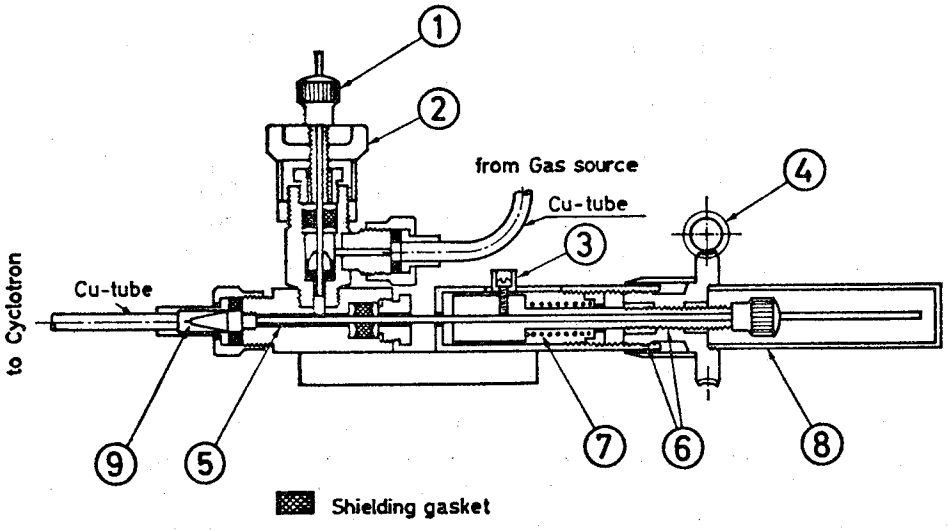

Fig. 3–7. Structure of needle valve. 1. Shaft chuck, 2. Stop valve, 3. Guide, 4. Worm, 5. Needle valve shaft, 6. Differential screw (pitch of 0.115 mm), 7. Spring, 8. Cover, 9. Needle. From [69–7].

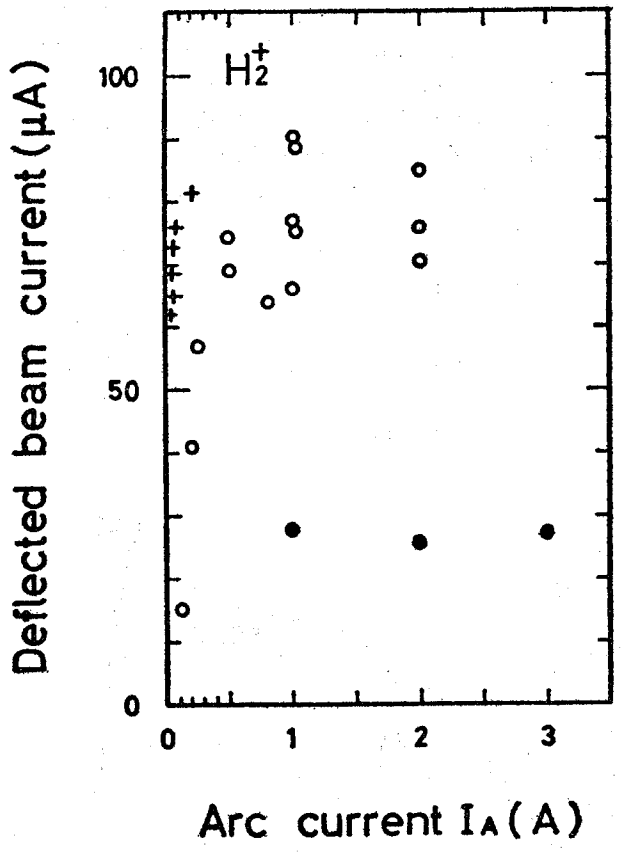

Fig. 3–8. Deflected beam current *vs.* arc current. Ion is H_2^+
●: V_{arc}=50 V, ○: V_{arc}=100 V,
+: V_{arc}=100 V (after a few days operation).
$\Delta p = 0.45 \times 10^{-5}$ Torr for all cases. From [69–7].

is of an ordinary type and therefore the beam focusing is weak, but such high intensity beam was obtained by the improvement of the ion source.

IV. HEAVY ION ACCELERATION AND COULOMB EXCITATION EXPERIMENT

Co-operating with the members of the Department of Nuclear Engineering, Faculty of Engineering, heavy ion acceleration by the cyclotron has been tried since 1963. Some preliminary results were described in the decennial report of the past decade. Detailed report on the heavy ion acceleration was published in 1967 [67–14], and Coulomb excitation of some medium heavy nuclides were investigated by the use of the accelerated heavy ion beams [67–13].

In those days, the radio-frequency of the cyclotron was fixed, so the magnetic field must be adjusted to satisfy the resonance condition. By replacing the materials of ion source so as to produce as highly ionized particle as possible, and shimming the magnetic field to give focusing actions, they succeeded in the acceleration of C^{2+} ions

and N^{3+} ions. These heavy ions were accelerated by third subharmonic mode and the beam current of 100nA was extracted from the cyclotron. Figure 4–1 shows the probe current *vs.* radius for different magnet current. The ions are of N^{3+}. The structure of the probe is shown in Fig. 4–2. This current probe was designed to receive ion beams with the width of 5 mm and can detect the turn separation of the beam. Other than the third subharmonic acceleration, the fifth subharmonic acceleration was observed.

By the use of thus accelerated N^{3+} ions, Coulomb excitations of ^{45}Sc, ^{75}As, ^{127}I and ^{133}Cs were studied [67–13]. The energy of the ^{14}N ions was 11.5 MeV. The experimental layout is shown in Fig. 4–3. As seen from this figure, de-excitation gamma rays were measured during beam bombardment. Since the target was thick, they corrected the effect of energy loss of nitrogen ions in the target. They obtained the B(E2) values from the experiment. The results are shown in Table IV–1. These

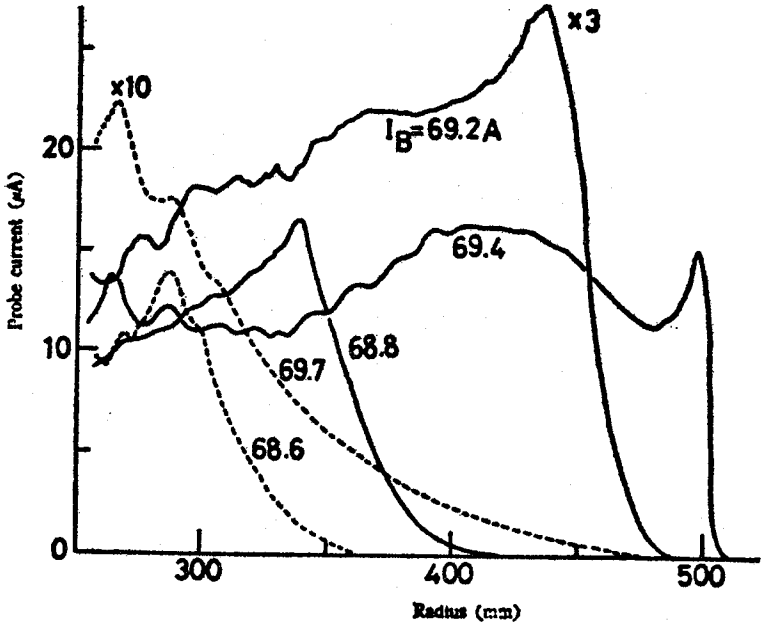

Fig. 4–1. Probe current *vs.* radius for different magnet current I_B, two shims of radius 42 cm and thickness 1 mm were installed. From [67–14].

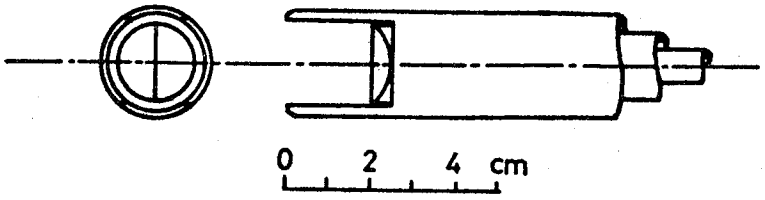

Fig. 4–2. Schematic view of the probe electrode used to measure internal beam intensity of heavy ions. Material is water-cooled copper. From [67–14].

works were the pioneering works in Japan and the construction of heavy ion Van de Graaff accelerator of the Department of Nuclear Engineering was promoted by these investigations.

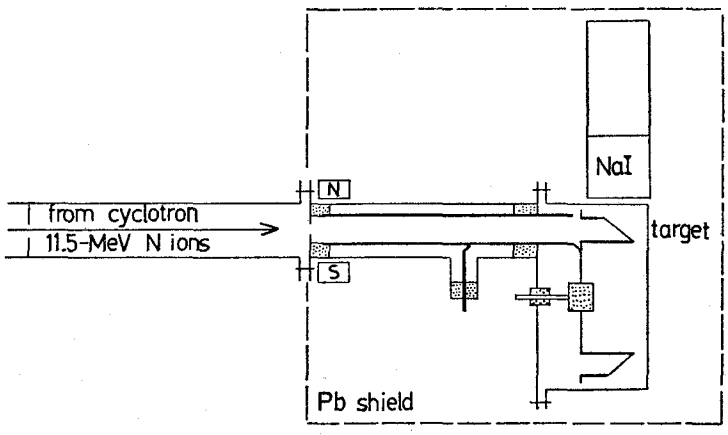

Fig. 4–3. Schematic view of the target chamber and detector arrangement. From [67–13].

Table IV–1. Gamma Ray Yields and B(E2) Values From [67–13].

Nucleus	Target material	Level (keV)	Measured Y/I	Number of incident particles $I\times10^{13}$	εB(E2) ↑ (e^2b^2)	Internal conversion coefficient α	B(E2) ↑ c) (e^2b^2)
^{45}Sc	Sc_2O_3	378	3.9×10^{-9}	3.0	0.0086	<0.01[a]	0.0086
^{75}As	As	280	1.6×10^{-8}	3.3	0.050	0.01[b]	0.051
		199	1.3×10^{-8}		0.015	0.02	0.015
^{127}I	CuI	203	3.0×10^{-9}	6.0	0.060	0.1[b]	0.072
		59	6.2×10^{-9}		0.011	3.9	0.054
^{133}Cs	$CsNO_3$	160	7.9×10^{-10}	4.4	0.011	0.34[b]	0.13
		81	2.3×10^{-9}		0.008	1.7	0.022

a) The transition to the 12 keV level.
b) The transition to the ground state.
c) An error of 20% is assigned to B(E2).

V. TARGET PREPARATION

The methods of target preparation are described briefly in the preceding decennial report. In 1969, details of the vacuum evaporator for target preparation was reported by Y. Uemura *et al.* [69–8]. Figure 5–1 shows the diagrammatic view of this evaparator. With this evaporator, thin foils of almost all solid substances could be produced in our laboratory. Target materials hitherto processed are Li, LiF, Be, B, C, LiF, Na, Mg, Al, Si, S, Cs, Sc, Ti, V, Cr, Mn, Fe, Cu, Zn, Ge, As, Se, Zr, Ag, Cd, Sn, Au, Pb, and Bi.

When a particle-particle correlation experiment is studied, conventional gas target is inconvenient and CD_2 film was used as deuteron target for an example. However, a very thin gas chamber sandwiched by two Havor foils was developed and used as ^3He or ^4He target for coincidence experiment.

For the measurement of excitation function of deuteron induced reactions, chemical preparation is of importance. Target chemistry of Ruthenium is reported by K. Komura *et al.* in this decade [69–5].

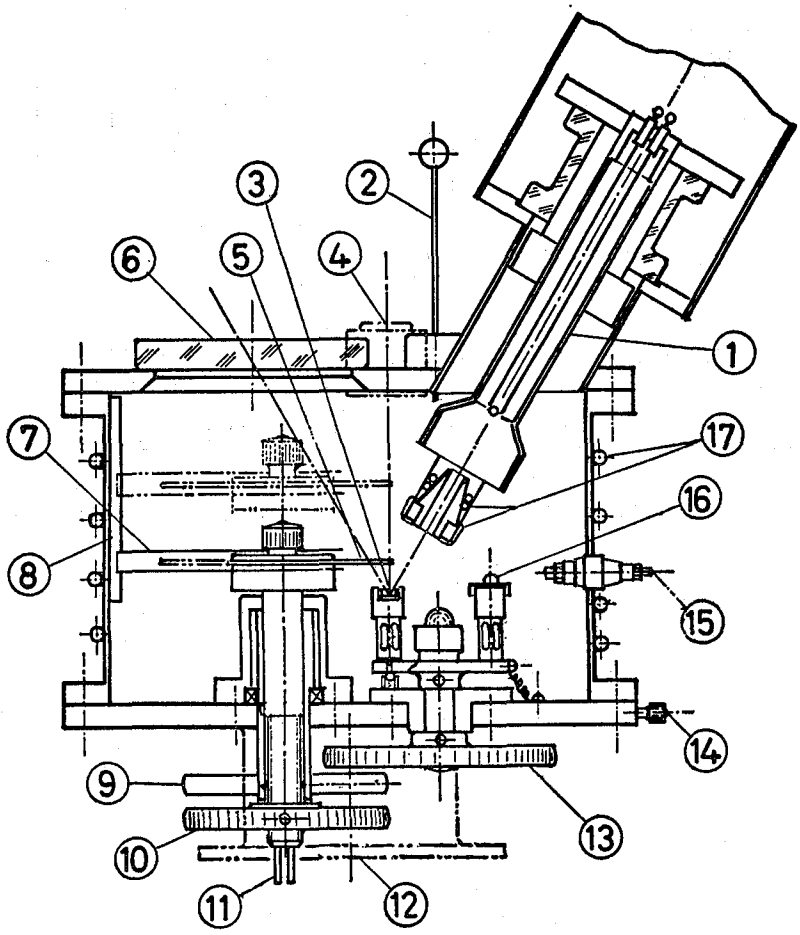

Fig. 5–1. Schematic view of the evaporation chamber, vacuum seals omitted. 1. Electron gun, 2. Hook, 3. Melting pot, 4. Box for a liquid nitrogen vessel to cool a substrate holder (not shown in the figure), 5. Substrate holder, 6. Window, 7. Shielding box of the substrate table, 8. Guide pipe, 9. Handle, turning, 10. Handle, up and down, 11. Cooling pipe, 12. Exhaust tube, 13. Handle, turning, 14. Terminal to ground, 15. Terminal, up to 70A, 16.Cap of the pot, 17. Cooling pipes. From [69–8].

VI. ELECTRONICS AND DATA PROCESSING

Electronic and logic circuits necessary for nuclear physics experiments were all hand made in the past decade. Gradually, the commercial based circuits for nuclear physics became available and the needs for circuit design and construction decreased in this decade. However, special type circuitry which accomodates the conditions of experiments by using the beam of cyclotron was developed in our laboratory.

Two papers were published in this decade. One concerns with the fast coincidence circuits [69–6], and the other with the time-of-flight measurements [70–2]. Because the beam from the cyclotron is of a bunched form which repeats every 77 ns, therefore, if the particle-particle correlation was measured, all data taking must be finished within 77 ns. Moreover, to lessen the random coincidence background, the coincidence width should be much more narrower than 77 ns. Fukunaga *et al.* [69–6] developed transistorized circuits for the coincidence experiments, and the characteristics of the circuits are listed in the following. Besides the circuits listed, linear gate circuit and pulse stretcher were also developed but explanations are omitted. These circuits were used successfully for the three body reaction experiments until 1972 or so. Figure 6–1 shows the block diagram of the type 1 coincidence circuit as an example.

circuit	type	spec.	noise level
preamplifier	high input impedance	risetime 5ns	1 mV
linear amplifier	monopolar, feed back	risetime 4ns	
	bipolar	risetime 10ns	
discriminator	type 1	delay time 30ns	
	type 2	delay time 75ns	
coincidence circuit	type 1	resolving time sum of input pulses	
	type 2	resolving time determined by delay line clipping	

Time-of-flight measuring circuit was developed to detect and identify heavy product particles. As described in the introduction of [70–2], cluster structure of light nuclei has been investigated in our laboratory for more than 10 years. Cluster structure studies include cluster pickup reactions, and then a need for heavy product particle detection arose. To detect the heavy particle, time-of-flight method coupled with a total energy detection is most useful and does not suffer from the change of charge state of heavy ions. Yasue *et al.* developed a time-of-flight circuit of time resolution 1.5 ns for the use of heavy particle production experiments. Figure 6–2 shows the circuit diagram of the time to pulse height converter. Figure 6–3 shows

the energy spectrum of particles obtained in a preliminary experiment. Protons, deuterons and carbon ions are separated clearly. As a byproduct, in the course of developing this time-of-flight method, the intensity variation of the cyclotron beam

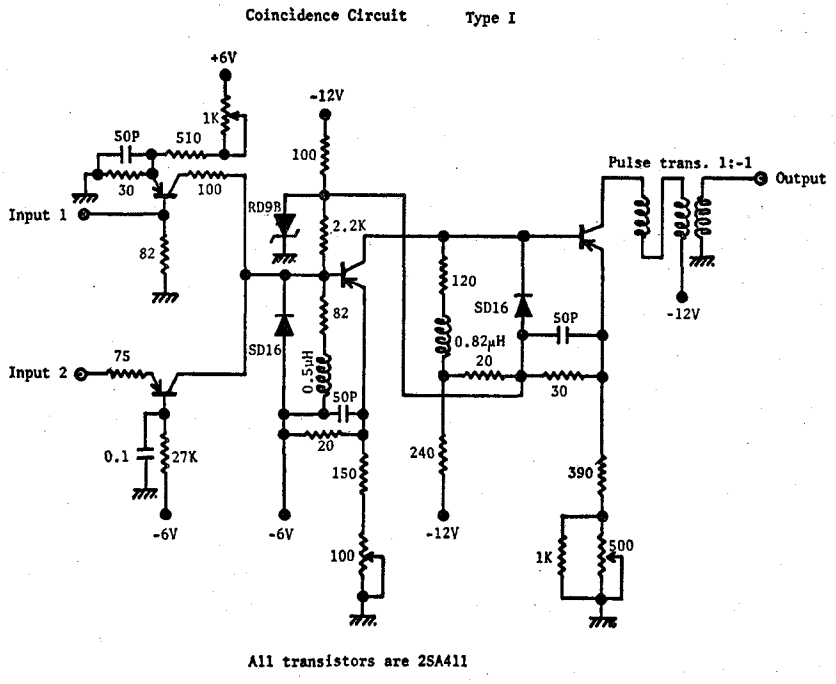

Fig. 6–1. Circuit diagram of the coincidence circuit of type 1. From [69–6].

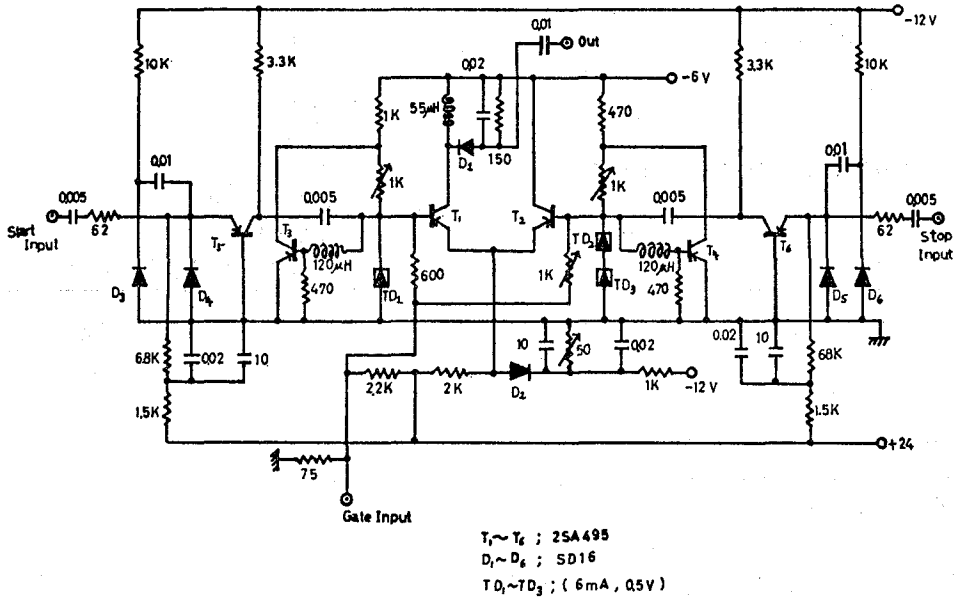

Fig. 6–2. Circuit diagram of the time to pulse height converter. From [70–2].

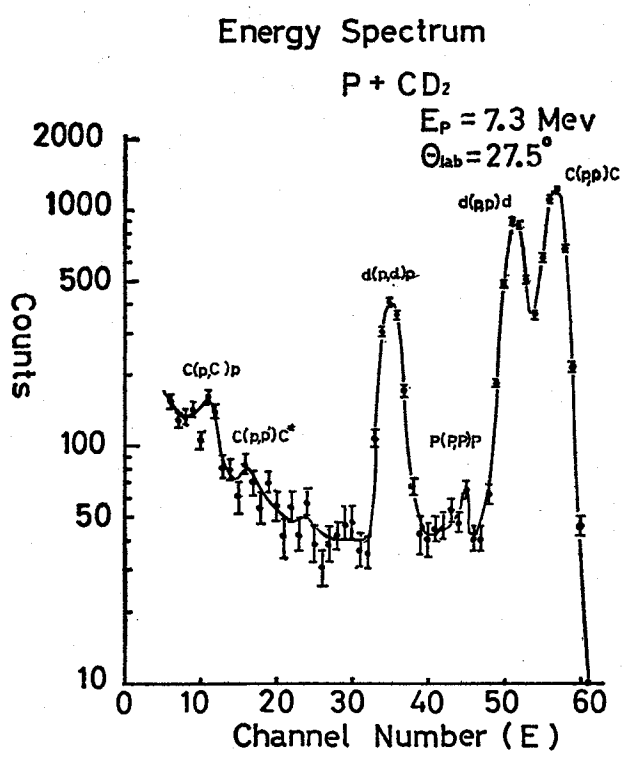

Fig. 6–3. Energy spectrum of products identified with a T-0-F method. Reaction, $p+CD_2$. From [70–2].

was clarified. As seen in Photo. 2 of [70–2], the cyclotron beam is modulated by 120 Hz repetition due to the ripple of the arc voltage of the ion source and by 360 Hz repetition due to the ripple of the d.c. power supply of R. F. accelerating voltage. In the design work of the cyclotron improvement, which is described in section III, care was taken to reduce the ripple of these power supplies.

The most astonishing change of the method of investigations between the preceding and this decade will be the spread of the computer. At early stage of this decade, in 1965 or so, computers were installed to every university as a central machine. Today, a mini-computer is included as an essential component of the experimental setup and on line data processing is quite usual. In our laboratory, Kokame developed a data processing program for the KDC–1 computer, which was installed in Kyoto University for the first time in 1965, to analyze automatically the singles spectrum of reaction products. Since the KDC–1 computer had only 4 kW memories, his program was written in machine language. Kokame's code was able to make automatic search of peaks in the spectrum, a proper background subtraction and calculations of differential cross sections in the laboratory system or in the center-of-mass system [66–5]. Later on, in 1973, a mini computer YHP 2100A was installed

in our laboratory and then in 1974, a medium sized FACOM 230–48 was installed in the computer center of the Institute for Chemical Research. Since these years, the investigation of the on-line data processing was promoted earnestly in our laboratory. The reasons were manyfolds. First, as described in section XIII, three body reactions have been the main item in our laboratory. In these investigations, particle-particle correlation measurements were inevitable, but one could get only crude data if a two dimensional pulse height analyzer is used because of the limitations of memory capacity. Second, in these investigations, particle identification is also inevitable. For this purpose, at least two kinds of informations are necessary to identify the particle, therefore, in the particle-particle correlation experiments, at least four kinds of informations must be processed within a very short time. If the detected particles are more than two kinds, more than 4 parameter data must be acquisited. Third, according to the diversity of data, to read out and to display these data manually become erroneous and almost impossible. From these reasons, on-line data acquisition and automatic data processing systems were developed earnestly in our laboratory. One of these efforts, multi-parameter data acquition system, was reported in this decade [76–1]. Figure 6–4 shows the flow chart of multiparameter event recorder and Fig. 6–5 shows the CRT display of the elastic p-d scattering. As seen from Fig. 6–5, the background is negligible. Further on-line data processing system are now in progress.

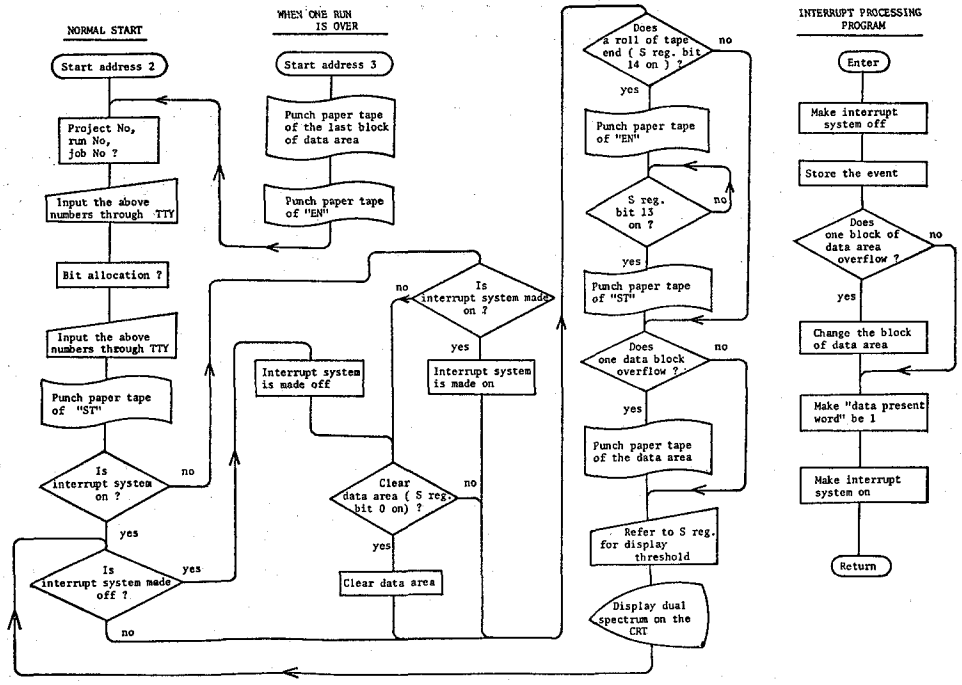

Fig. 6–4. Flow chart of the multi-parameter event recorder program. From [76–1].

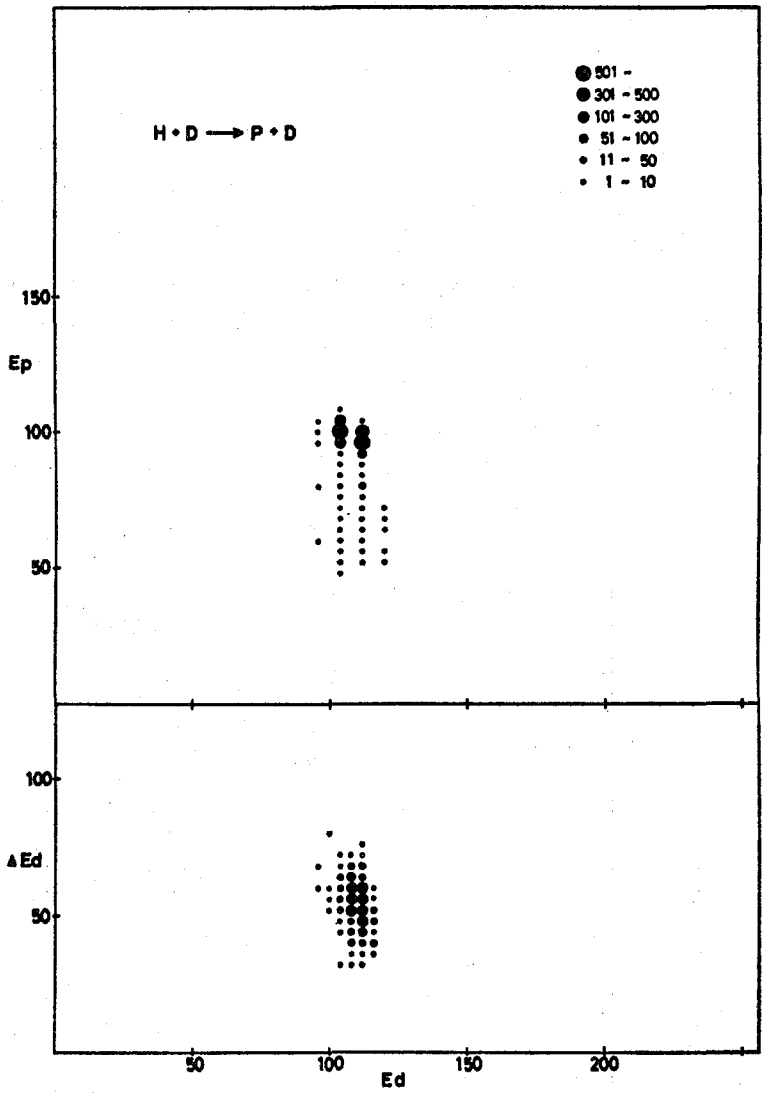

Fig. 6–5. Two dimensional display of p-d scattering events. From [76–1].

VII. INSTRUMENTATIONS FOR NUCLEAR RESEARCH

Three articles are published about instrumentations. One paper describes the beam tranport system [69–9]. Another paper reports the design and performance of a broad range magnetic spectrograph [69–10]. Remaining one concerns with the description of a scattering chamber for three body nuclear reactions [69–11]. Among these instrumentations, beam transport system and a broad range magnetic spectrograph were constructed before 1965, and merely the publications were delayed until 1969.

Beam transport system of the cyclotron consists of quadrupole lens magnets, a steering magnet and a beam momentum analyzing magnet.

Quadrupole magnet has an aperture of 12 cm; this opening was the largest one ever constructed in those days. Due to the pole shape of rectangular hyperbola, the quality of magnetic field is excellent and the field gradient is uniform within 0.1% up to 80% radius of mechanical opening. This behavior is shown in Fig. 7–1. The maximum field gradient is 600 Gauss/cm. This value is sufficient to focus the beam from the cyclotron at the source point of the momentum analyzing magnet.

The momentum analyzing magnet was designed to limit the momentum spread less than 0.05% when the source width was 1 mm wide. The curvature radius was chosen as 80 cm, but the experimentally determined value was 78.90 cm; 1 cm less than the designed value. This difference was due to the over-cutback of the fringing field correction. This experience was taken into account when the broad range magnetic spectrograph was designed. The dispersion of the analyzing magnet was almost equal to the designed value, and a beam of high precision energy was successfully brought to the reaction chamber of the magnetic spectrograph. Figure 7–2

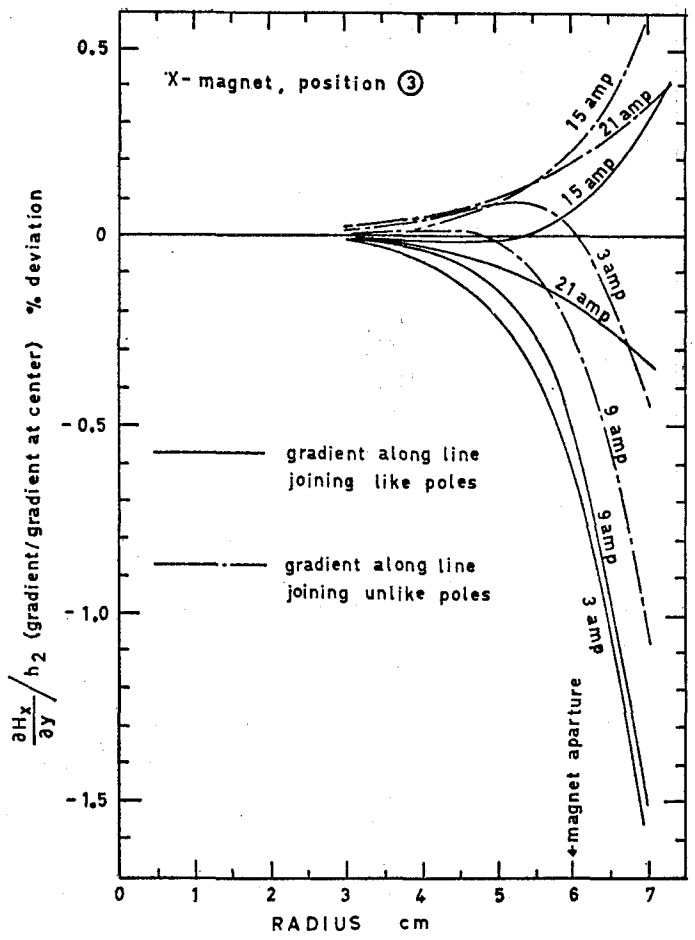

Fig. 7–1. Field gradient of a quadrupole magnet as functions of exciting current and of radius from center. Measured at center position of the magnet. From [69–9].

shows the dimensions of the analyzing magnet and Fig. 7–3 shows the radial direction distribution of its magnetic field. The field distribution is uniform within the error of 1×10^{-4} in the effective range of the magnet.

Broad range magnetic spectrograph is of a Browne-Buechner type. The cut-away view of this spectrograph is shown in Fig. 1 of [69–10]. Specifications of the

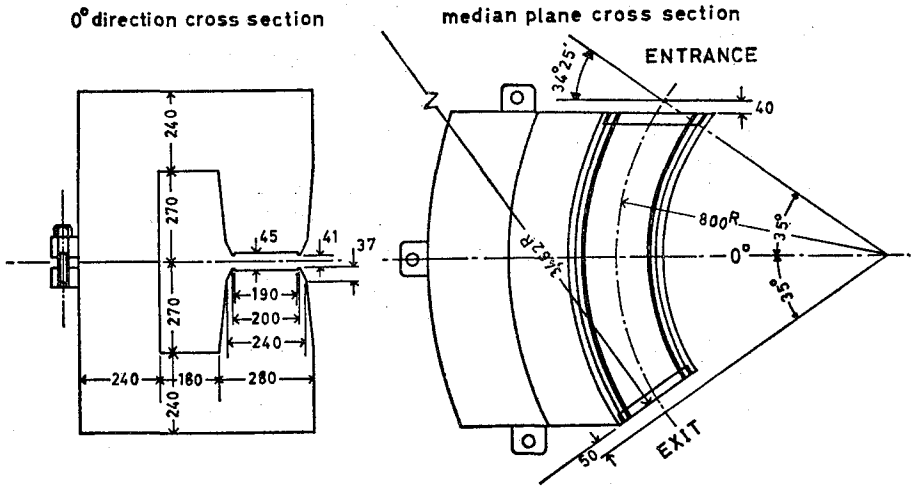

Fig. 7–2. Dimensions of the beam momentum analyzing magnet. From [69–9].

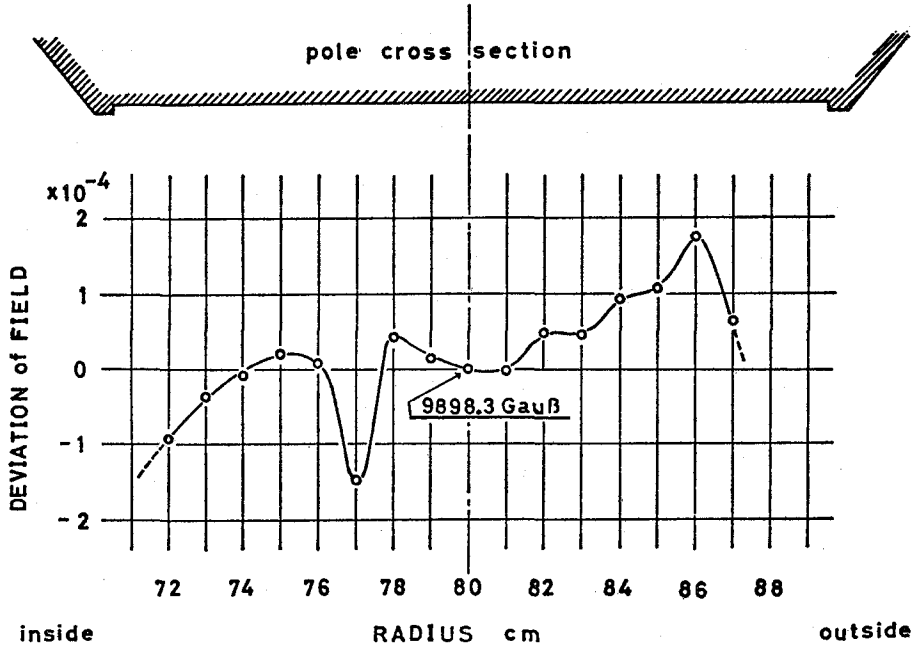

Fig. 7–3. Radial direction distribution of the momentum analyzing magnet. Normalized to the value at center. From [69–9].

Table VII–1. Specifications of a Broad Range Magnetic Spectrograph
From [69–10]

maximum to minimum energy ratio	1:0.3989
effective pole radius R	670 mm
range of beam radius	0.60 R to 0.95 R
maximum detectable momentum	9.0×10^5 Gauss-cm
maximum particle energy	46 MeV α and p, 23 MeV d
magnet pole gap	20 mm
magnet main coil	2784 turns. 22000 AT
magnet auxiliary coil	800 turns. 400 AT
entrance angle ε_1	35°
exit angle ε_2	0°
magnification	0.469 at 0.60 R
	1.66 at 0.95 R
curvature for second order focusing	R_1=443.3 mm
	R_2=670.0 mm
maximum solid angle	1.451×10^{-3} sterad
focal length	163.5 mm at 0.60 R
	851.8 mm at 0.95 R
minimum momentum resolution	0.05% at 0.80 R and
	with source width 1 mm

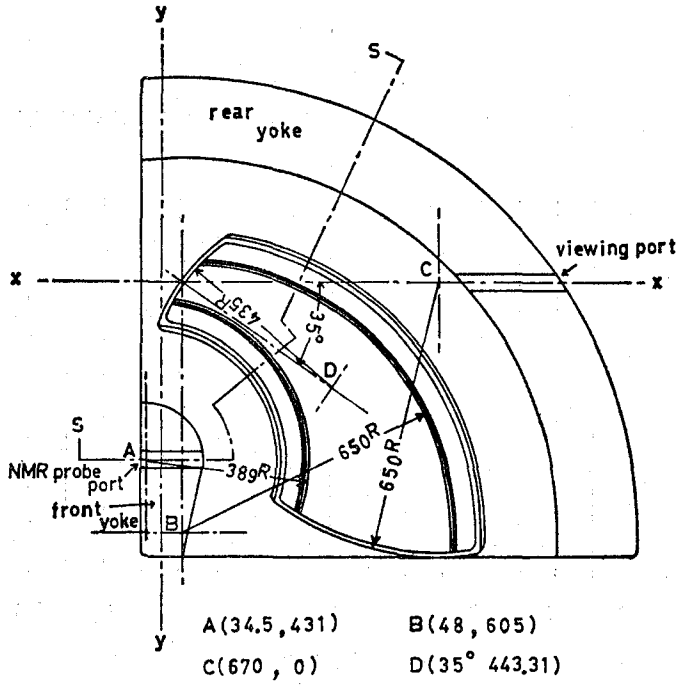

Fig. 7–4. Dimensions of the spectrograph magnet. Symbols A, B, C, and D indicate the center positions of curvature. From [69–10].

spectrograph are listed in Table VII–1, and the dimensions of the magnet is shown in Fig. 7–4. This broad range magnetic spectrograph was used in the investigations of (d,p) stripping of deuterons [66–6], elastic and inelastic scattering of deuterons [66–6], (α,d) reactions [65–14] and stopping power measurements [65–16]. Design work was made to get energy resolution less than 0.1% at most favorable focusing point. This value was successfully achieved and precise assignments of many levels were carried out without suffering from the background.

As described in section XIII, three body nuclear reaction is one of the main items in our laboratory. In the early stage of the experiments, an old scattering chamber was modified to detect the particle-particle coincidences in the horizontal plane, but because this chamber was very inconvenient for three body reactions, a new scattering chamber was specially designed and constructed [69–11]. This chamber is equipped with one rotating ring and two movable arms, (frequently we call it

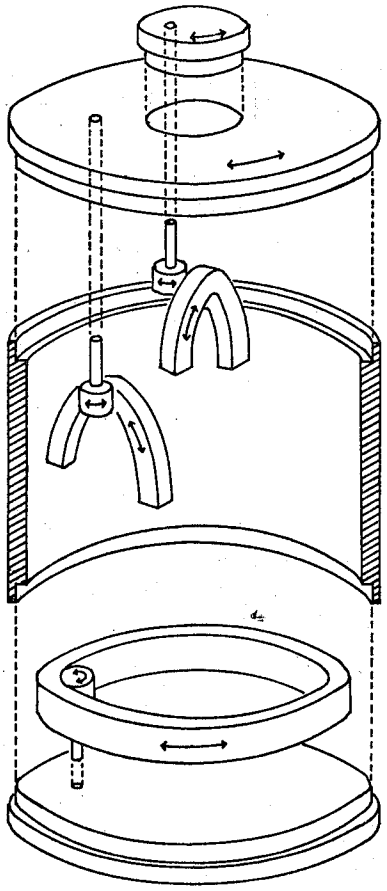

Fig. 7–5. Schematic drawing of the principle of three-dimensional freedom and three sets of moving arms. From [69–11].

"Bogen"). By equipping the detectors to these "Bogen", one can detect particles emitted to any direction in three-dimensional space. The principle of this three dimensional freedom is shown in Fig. 7–5. By the use of this chamber, one can investigate the particle-particle correlation not only in the reaction plane but also off the reaction plane. For example, one can detect the particles emitted in a cone of which the axis is in the direction of the recoil center of mass. Almost all the experiments explained in section XIII were carried out by using this chamber.

VIII. STOPPING POWERS OF VARIOUS MATERIALS

Stopping powers of materials against the charged, high speed particles are the old and new problem of nuclear physics. In our laboratory, precise measurements of stopping powers of Sn, Au and Mylar for 28 MeV alpha particles were carried out in 1965 by using the broad range magnetic spectrograph which was then just in operation. This work has been continued under the leadership of Professor R. Ishiwari, who moved from our laboratory to the Department of Physics of Nara Womens University. According to a formula presented by Livingston and Bethe in 1936, the stopping power of charge Z material is

$$-\frac{dE}{dx}=\frac{4\pi z^2e^4}{mv^2}\cdot NZ\left\{log\frac{2mv^2}{I}+log\frac{1}{1-\beta^2}-\beta^2-\frac{\sum_i C_i}{Z}\right\}$$

Here v is the velocity of incident particle, ze the charge of incident particle, N the number of atoms per cubic centimeter, m the rest mass of the electron, I the mean excitation potential of the atom, β the ratio v/c, and C_i the correction term which represents the deficit of the stopping power due to the ineffectiveness of the inner shell electrons. The aims of the experiments of Ishiwari *et al.* are

1) If this formula is exact, the stopping power of material should be dependent only on ze and v. Then, the stopping power of a material should be quite equal for protons and deuterons of the same velocity. How the measured values of stopping powers coincide or deviate from the theoretical predictions?

2) Many experiments have been carried out by many authors since 1936, but still the exact values of I and C_i are not decisively determined. Therefore, precise measurement is hoped to determine these values.

3) Stopping power of materials differs each other when the measurements were made by different authors and by different apparatus. Therefore, it is necessary to get standard values of stopping power of materials and unify the values hitherto obtained.

Ishiwari *et al.* in collaboration with the Nuclear Science Research Facility, have made efforts to get precise values of stopping powers of various materials within the absolute error of 0.1% by using beams of protons, deuterons, and alpha particles from the Kyoto University Cyclotron. Five papers were published during this decade, [67–15], [71–1], [71–2], [74–3], and [74–15]. Important results they got are in-

troduced briefly in the following. Figure 8–1 shows the experimental arrangement they used. A beam from the cyclotron are deflected magnetically and its velocity is determined with the aid of two slit system. The curvature of the beam path is calibrated exactly by using the standard alpha source Th(C+C′). The energy of the beam and consequently the velocity of the beam was defined within the error of 0.002 percent. The beam is scattered from a gold foil at the center of the scattering chamber and an absorber is inserted between the target foil and a detector. Some of the results obtained are listed below.

In Table VIII–1 are listed the stopping powers of aluminum for protons and deuterons of exactly the same velocity. The energies of incident protons and deuterons are 7.1756±0.0017 MeV and 14.3698±0.0029 MeV respectively. From this table, it is seen that the stopping power is the same for deuterons and for protons of

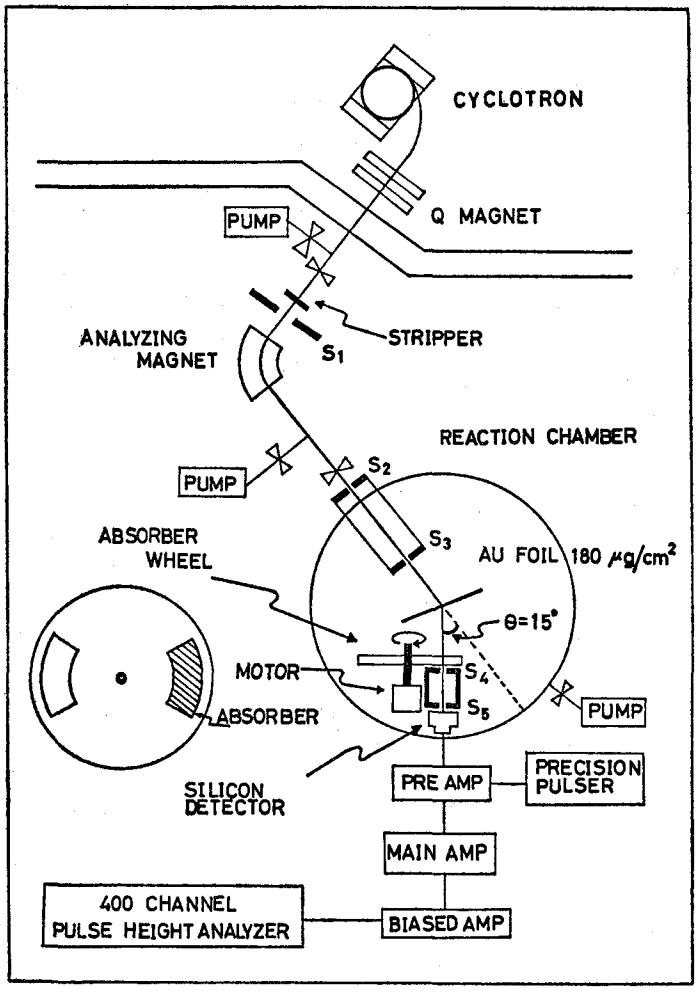

Fig. 8–1. Experimental arrangement for the energy loss measurement. From [74–3].

Table VIII-1. The average values of incident energies and energy losses for protons and deuterons of exactly the same velocity. The absorber is Al. Figures in the parenthesis are the fractional errors. All errors are standard errors. The fractional difference for protons and deuterons for each absorber are also shown. From [67-15].

Particle	Incident energy (keV)	Energy losses and Fractional error (%)	
		17 microns	37.5 microns
proton	7269.78±2.11	197.42±1.45 (0.73)	447.25±2.04 (0.46)
deuteron	14515.95±1.63	197.38±0.86 (0.44)	444.70±2.58 (0.58)
Difference		0.04±1.69	2.55±3.29
Fractional Difference (%)		0.020	0.50

Table VIII-2. Comparison of Nara data with Anderson's data. All data have been reduced to 7.0 MeV. Data of Ni and Pt are taken from [71-2]. Data for Al, Cu, Ag, and Au are average values of [74-3] and [71-2]. For other references, please refer [74-3].

Element	Nara Data (keV/mg cm^{-2})	Anderson *et al.*** (keV/mg cm^{-2})	Difference (%)
Al	43.62±0.15	44.81±0.13	−2.73±0.46
Ti	37.65±0.17	38.92±0.12	−3.37±0.55
Fe	36.18±0.16	37.28±0.11	−3.04±0.53
Ni	36.16±0.19	37.29±0.11	−3.13±0.61
Cu	34.50±0.12	35.12±0.11	−1.80±0.46
Ag	28.98±0.11	29.48±0.09	−1.73±0.48
Ta	23.08±0.11	23.66±0.07	−2.51±0.56
Pt	22.20±0.12	22.54±0.07	−1.53±0.63
Au	22.26±0.09	22.67±0.07	−1.84±0.51

* Ref. 7).
** Ref. 4), 5), 6).

the same velocity. Table VIII-2 shows the comparison between the values for protons obtained by Ishiwari *et al.* and those of Anderson *et al.* As seen in the table, Nara data give slightly lower values than those of Anderson *et al.* Where this difference come from, is an important problem.

Ishiwari *et al.* gave more sophisticated discussions about this phenomenon and also the problem of shell correction, mean ionization potential and the oscillatory behavior of Bloch constants. Their work is excellent and gives firm foundation of the stopping power of various materials.

IX. ELASTIC AND INELASTIC SCATTERING OF ALPHA PARTICLES

Elastic and inelastic scattering of alpha particles from nuclei by using the Kyoto University Cyclotron were investigated continuously in this decade. Scattering of alpha particles has characteristics such that the alpha particle excites preferentially the collective mode of the nucleus and behaves as if a simple, point like nucleus. Therefore, by the method of inelastic scattering, one could excite fairly high excited states even with low energy alpha particle beam. Supported by the progress in

DWBA analysis and in computational method, plenty of informations about the nuclear structure was obtained in this decade.

Nuclides and excited states investigated are as follows. Among these nuclides, light ones were investigated by staff members of Kéage Laboratory and medium-heavy nuclides by staff members of the Department of Physics. In light nuclei, attention was paid to investigate the deviations from the collective excitation model such as the cluster structuer of ^{9}Be, the spin flip state excitation in ^{12}C, ^{24}Mg, and ^{28}Si, unnatural parity state of ^{12}C, ^{24}Mg, and ^{28}Si, vibrational 3^- states in ^{24}Mg and ^{28}Si. In medium-heavy nuclei, it was the aim of investigation to get good fit parameters of DWBA analysis and to get quadrupole deformation parameter (β_2) and octupole deformation parameter (β_3).

Nucleus	Investigated States	Reference
^{9}Be	g'nd, 1.7, 2.43, 3.04 MeV	[67–6]
^{11}B	g'nd, 8.6 MeV	[67–4]
^{12}C	g'nd, 11.8, 12.7, 14.08 MeV	[67–4]
^{24}Mg	g'nd, 1.37, 8.4 MeV	[66–2]
^{24}Mg	g'nd, 5.22, 10.4 MeV	[67–7]
Mg	g'nd,	[74–10]
^{28}Si	g'nd, 1.77, 6.88 MeV	[66–2]
^{28}Si	g'nd, 8.9 MeV	[67–4]
^{28}Si	g'nd,	[74–10]
^{32}S	g'nd,	[74–10]
^{40}Ar	g'nd,	[74–10]
Ti	g'nd, 0.99, 1.55, 2.35, 3.34, 4.02, 4.57 MeV	[66–1]
^{58}Ni	continuum state	[67–5]
^{64}Ni	g'nd, 1.34 MeV 3.52 MeV	[68–8]
^{65}Cu	g'nd, 0.770, 1.114, 1.482, 1.623, 1.725,	
	2.093 MeV quadrupole state	[68–8]
	2.52, 2.85, 2.98, 3.08, 3.35, 3.50,	
	3.72, 4.05 MeV octupole state	[68–8]
Cu	g'nd, 0.68, 0.99, 1.35, 1.82, 2.03 MeV	[66–1]
Ag	g'nd, 0.37, 0.9, 2.10 MeV	[66–1]
Cd	g'nd, 0.58, 1.22, 1.92 MeV	[66–1]
Sn	g'nd, 1.21, 2.41 MeV	[66–1]
Ta	continuum state	[67–5]
Au	continuum state	[67–5]

First, we introduce the excited states and their deformation parameters obtained in Table IX–1. An example of good fit of DWBA analysis to the elastic scattering of alpha particle is shown in Fig. 9–1. This work was done by Kokame recently and the parameters used are listed in Table IX–2, and an example of DWBA fit to the inelastic scattering is shown in Fig. 9–2. Generally, DWBA fit becomes better in heavier nuclei than light nuclei. Besides, non-phonon excitations such as spin flip excitation and particle unstable state excitation are observable in light nuclei. Nakamura

Table IX–1.

Nuclide	Exc. Energy (MeV)	J^π	$\|\beta\|$	β_2	β_3	Ref.
^{9}B	2.43	$5/2^-$	0.38			[67–6]
^{24}Mg	1.37	2^+		0.35		[66–2]
	8.4	3^-			0.22	[66–2]
^{28}Si	1.77	2^+		0.29		[66–2]
	6.88	3^-			0.28	[66–2]
^{64}Ni	3.52	3^-			0.154	[68–8]
^{65}Cu	0.770	$1/2^-$		0.174		[68–8]
	1.114	$5/2^-$		0.181		[68–8]
	1.482	$7/2^-$		0.173		[68–8]
	1.623	$5/2^-$		0.055		[68–8]
	1.725	$1/2^-$		0.084		[68–8]
	2.093	$3/2^-$		0.097		[68–8]
	2.52	3^-			0.154	[68–8]
	2.85	$9/2^-$			0.172	[68–8]
	3.35	$(5/2^+)$			0.150	[68–8]
Ag	0.37			0.21		[66–1]
	0.90			0.06		[66–1]
	2.10				0.13	[66–1]
Cd	0.58			0.14		[66–1]
	1.22			0.04		[66–1]
	1.92				0.11	[66–1]
Sn	1.21			0.11		[66–1]
	2.41				0.13	[66–1]

Table IX–2.

Nucleus	E_α (Mev)	V_R (MeV)	W_I (MeV)	r_R (fm)	r_I (fm)	a_R (fm)	a_I (fm)	rc (fm)	θ_R (mb)	χ^2
Mg	28.4	55.95	10.56	1.72	1.77	0.520	0.450	1.4	1187	39.8
Si	28.3	51.72	10.87	1.69	1.48	0.540	0.679	1.4	1230	6.0

investigated spin-flip unnatural parity state excitation by alpha particle inelastic scattering. In this case, the spin-orbit interaction between an incident alpha particle and a nucleon in the target nucleus plays an important role. The angular distributions of alpha particles leaving the ^{12}C nucleus in its 12.7 MeV 1^+ spin-flip state and leaving the ^{11}B nucleus in its 8.6 MeV spin-flip state are shown in Fig. 9–3. The angular distribution does not show popular diffraction like pattern.

The correspondence between the deformation parameters and electromagnetic multipole transition strengths is discussed by Kumabe *et al.* and Kokame *et al.* and when the DWBA fit is good, the correspondence is also good.

Inelastic scattering of alpha particles leading to the continuum state of the residual nucleus is a phenomenon complementary to the inelasting scattering to

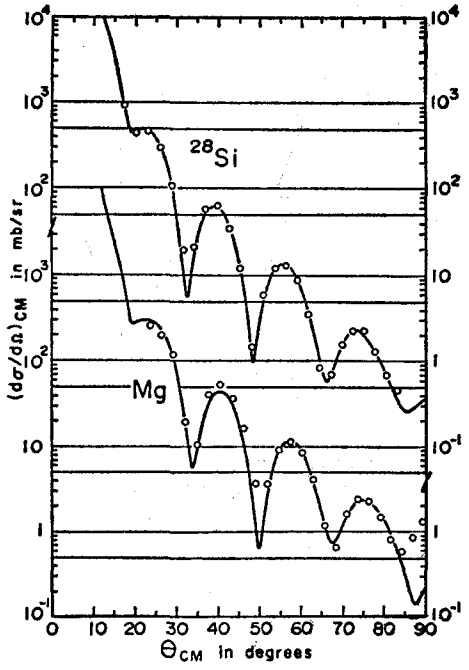

Fig. 9–1. Experimental (in open circle) and theoretical (in solid line) cross sections of elastic scattering of alpha particles from Mg and Si. DWBA parameters are listed in Table IX–2. From [74–10].

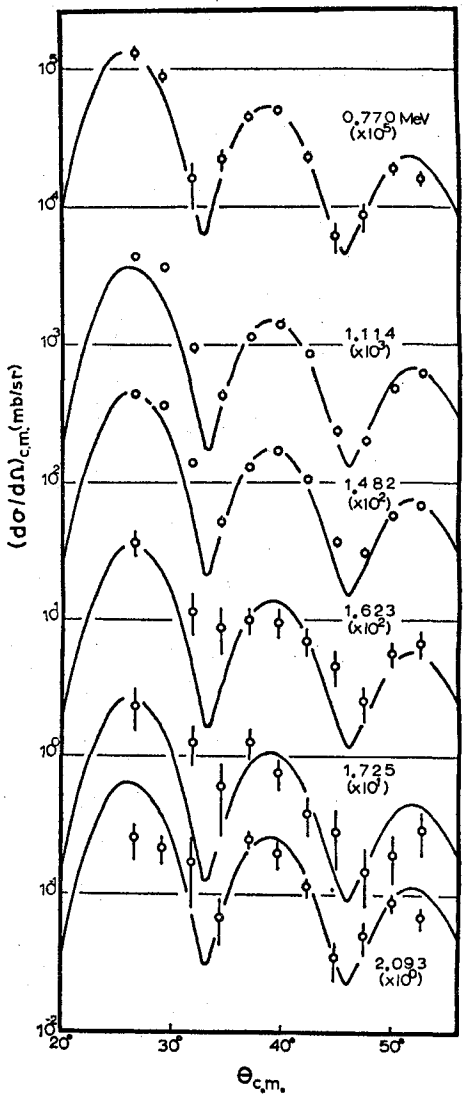

Fig. 9–2. DWBA fit to the quadrupole excitations of ^{65}Cu by inelastic scattering of 28 MeV alpha particles. Values of parameter β_2 are listed in Table IX–1. From [68–8].

discrete levels. The investigation was made by Kumabe *et al.* [67–5] under the condition that particles other than alpha particles escape through the detector. The continuous alpha particle energy spectra show various shapes but for ^{58}Ni and Ta, they obtained Maxwellian distribution and they suggested the nuclear temperature of the excited state. The result is shown in Fig. 9–4 for the case of Ag. It is interesting that such complex particle as an alpha particle is absorbed completely by

the nucleus and then evaporate as an alpha particle entity leaving the nucleus in continuum state. This fact shows that the inelastic scattering of alpha particles occur via various processes.

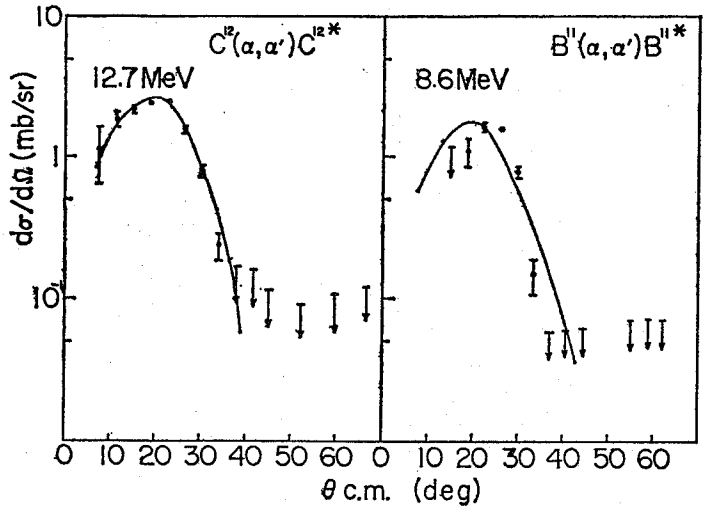

Fig. 9–3. Angular distribution of alpha particles leaving ^{12}C in 12.7 MeV spin-flip state and ^{11}B in 8.6 MeV spin-flip state. The solid lines are PWIA fit. From [67–4].

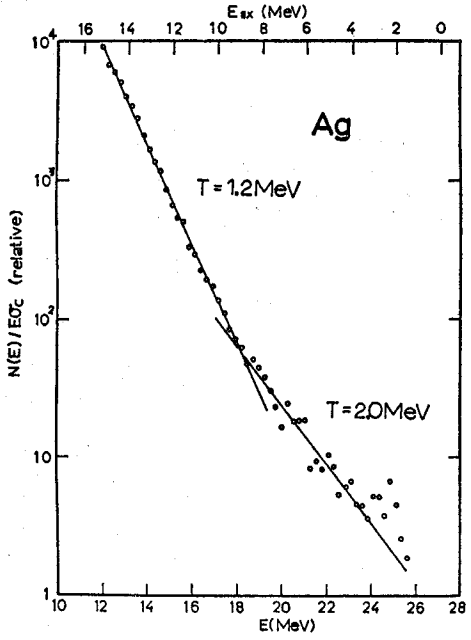

Fig. 9–4. Energy spectrum of alpha particles leaving Ag in its continuum state. The abscissa in the upper place represents the excitation energy of Ag, and the ordinate indicates the quantity $N(E)/E\sigma_c(E)$. From [67–5].

X. ELASTIC AND INELASTIC SCATTERING OF DEUTERONS

Deuteron is a very interesting particle. It is a very loosely bound nucleus such that one can think of it as if a neutron carrier or a proton carrier. In the past decade, deuteron stripping reaction was used to investigate the valence proton or neutron state on the basis of this loosely bound nature. On the other hand, deuteron is not so fragil as expected from its very small binding energy. High energy deuteron production is observed in the high energy proton-nucleus scattering with the same order of magnitude as the elastic scattering of protons. Proton-neutron pair correlation is thought to be very strong in the nucleus referring such experiments. Further, deuteron wave function is not yet decisive today, especially, the high momentum part of the deuteron wave function has much ambiguities. In our laboratory, scattering and reactions of deuterons were investigated continuously through past and present decade. Target nuclides and levels investigated are as follows.

Nucleus	Levels investigated	Reference
^{2}H	g'nd	[67–8], [68–11]
^{4}He	g'nd	[67–8], [68–11]
^{6}Li	2.18 MeV	[69–2]
^{7}Li	g'nd, 0.478, 4.63 MeV	[69–2]
^{9}Be	g'nd, 2.43 MeV	[66–6]
^{12}C	g'nd, 4.43 MeV	[66–6]
^{14}N	g'nd, 3.94, 4.91, 5.10 MeV	[66–6]
^{16}O	g'nd, 6.06, 6.14, 6.92, 7.12 MeV	[66–6]

d-d and d-α scattering was investigated by Itoh and preliminary results are already introduced in the past decade. Figures 10–1 and 10–2 show the optical

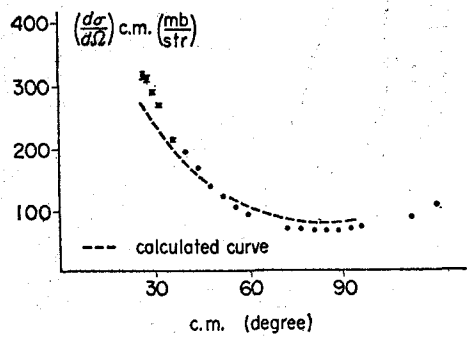

Fig. 10–1. The angular distribution of d–d elastic scattering at 14.2 MeV. The broken line shows the optical potential fit. From [68–11].

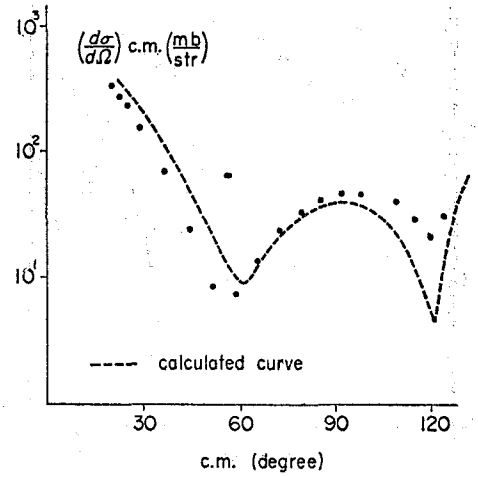

Fig. 10–2. The angular distribution of d-^{4}He elastic scattering at 14.2 MeV. The broken line shows the optical potential fit. From [68–11].

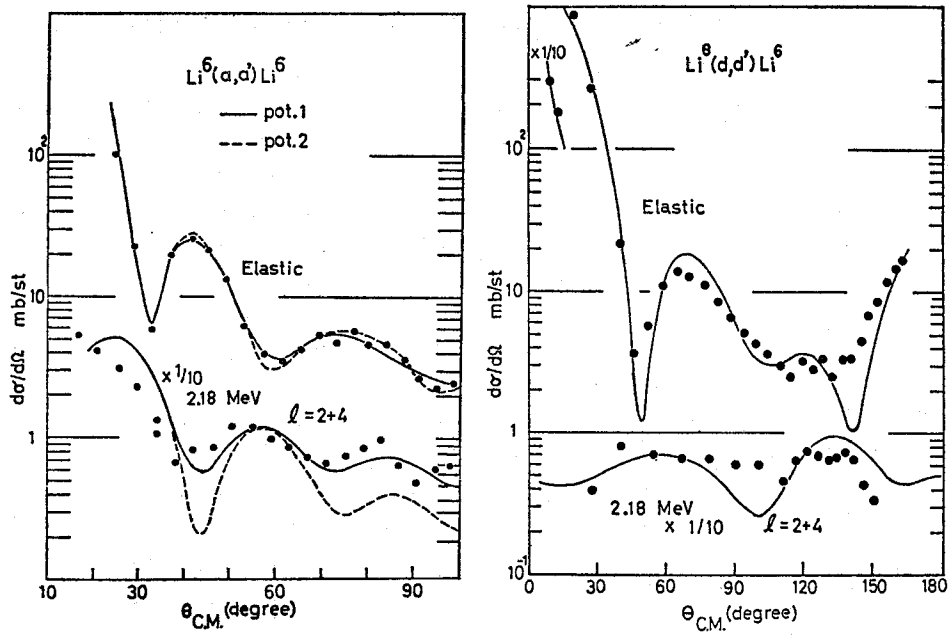

Fig. 10–3. The angular distributions of elastic and inelastic scattering of alpha particles and deuterons leading to the 2.18 MeV state of ^{6}Li. Solid lines are calculated curves with DWBA theory. From [69–2].

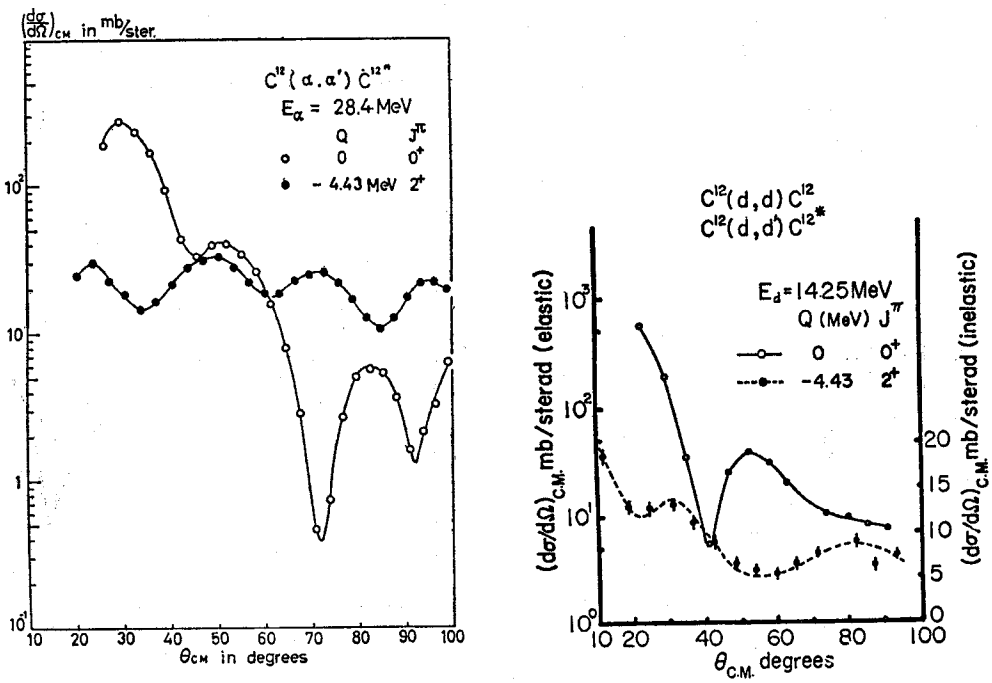

Fig. 10–4. Comparison of angular distributions of elastic and inelastic scattering of alpha particles and of deuterons from ^{12}C. The excitation of ^{12}C is 4.43 MeV. Left hand side figure from [65–4] in the preceding decennial report. Right hand side figure from [66–6]. The solid and dashed lines are the guide for the eye.

potential fit to the d-d and d-α scattering. Deviations from the optical potential fit are observed in the d-d scattering in the most forward angular range. This phenomenon is now being investigated further in our laboratory by observing the scattering in the more forward angular range.

Generally, angular distribution of inelastically scattered deuterons are more flat and sharp rise at forward angles diminish when compared to that of alpha particles. Matsuki investigated the deuteron and alpha particle scattering from ^{6}Li and ^{7}Li and the result is shown in Fig. 10–3. These characteristics are also observable when the targets heavier than Li are used. Figure 10–4 shows the comparison between the inelastic scattering of deuterons and of alpha particles leaving the ^{12}C nucleus in its 4.43 MeV state. Deuteron experiment was done by Nguyen and alpha particle experiment by Kokame.

DWBA fit for deuteron scattering is not so good as for alpha particle scattering. This difference may come from the fact that a deuteron wave function is more diverse than that of alpha particle, and one cannot treat the deuteron as a point like particle.

XI. DEUTERON INDUCED REACTIONS

Deuteron induced reactions were investigated in this decade following two approaches. One is the research of (d,p) reactions on light nuclei such as ^{12}C, ^{16}O, and ^{24}Mg to investigate the level scheme and the excitation mechanism of the residual nuclei. This work was done by members of the Kéage Laboratory. The other is the research of energy dependence of deuteron induced reactions on medium heavy elements. This work was done by members of the Department of Chemistry of Osaka University and of Research Institute for Atomic Energy of Kyoto University. Levels and types of reactions investigated are listed in the following table. The aim of the former experiment was to assign the spin-parities of levels of residual nuclei and to select out the j-forbidden (d,p) reactions. Hosono *et al.* carried out laborious experiment and analyses of data obtained by the use of the broad range magnetic spectrograph [69–10] and concluded that the j-forbidden (d,p) reaction occurs via two step process, that is, a neutron is captured by an excited core nucleus. Levels of the residual nucleus formed by a j-forbidden (d,p) reaction are listed in Table XI–1, and a typical angular distribution of protons leading to j-forbidden state is shown in Fig. 11–1.

They investigated further the (d,p) reaction leading to the particle unstable state. The ^{12}C(d,p)^{13}C reaction was taken as an object of research. They succeeded in observing the broad peak of protons leaving the residual ^{13}C nucleus in its 7.64 MeV and 8.33 MeV state. These states are particle unstable and decay into n+^{12}C with very short life times. Therefore, one can obtain the phase shifts of the neutron scattering by ^{12}C nucleus by analyzing the spectrum shape with the aid of final state interaction. The (d,p) stripping reactions leading to particle unstable state is a new field of research developed in this decade and Hosono *et al.*'s experi-

Target	Type of Reaction	Observed Quantity	Ref.
^{12}C	(d,p)	g'nd, 3.09, 3.68, 3.85, 6.86, 7.47, 7.53, 7.64, 8.33, 8.82, 9.50, 9.90 MeV state of ^{13}C	[67–12] [68–5] [70–3]
^{16}O	(d,p)	g'nd, 0.87, 3.06, 3.85, 4.56, 5.08, 5.22, 5.38, 5.70, 5.94, 6.87, 7.16, 7.28, 7.37, 7.56, 7.68 MeV state of ^{17}O	[68–5]
^{24}Mg	(d,p)	g'nd, 0.584, 0.976, 1.611, 1.962 MeV state of ^{25}Mg	[68–5]
^{64}Zn	(d,p)	yield of ^{65}Zn	[74–11]
	(d,n)	yield of ^{65}Ga	[74–11]
	(d,2n)	yield of ^{64}Ga	[74–11]
	(d,α)	yield of ^{62}Cu	[74–11]
	(d,αn)	yield of ^{61}Cu	[74–11]
^{70}Ge	(d,p)	yield of ^{71}Ge	[68–2] [69–12]
	(d,n)	yield of ^{71}As	[68–2] [69–12]
	(d,2n)	yield of ^{70}As	[68–2] [69–12]
	(d,α)	yield of ^{68}Ga	[68–2] [69–12]
^{76}Ge	(d,p)	yield of $^{77}Ge^{m}$	[74–11]
	(d,p)	yield of $^{77}Ge^{g}$	[74–11]
	(d,n)	yield of ^{77}As	[74–11]
	(d,2n)	yield of ^{76}As	[74–11]
	(d,α)	yield of ^{74}Ga	[74–11]
	(d,αn)	yield of ^{73}Ga	[74–11]
^{96}Zr	(d,p)	yield of ^{97}Zr	[68–2]
	(d,n)	yield of ^{97}Nb	[68–2]
	(d,2n)	yield of ^{96}Nb	[68–2]
	(d,3n)	yield of ^{95}Nb	[68–2]
^{96}Ru	(d,p)	yield of ^{97}Ru	[69–13]
^{102}Ru	(d,p)	yield of ^{103}Ru	[69–13]
^{104}Ru	(d,p)	yield of ^{105}Ru	[69–13]
^{130}Te	(d,p)	yield of ^{131}Te	[68–2]
	(d,n)	yield of ^{131}I	[68–2]
	(d,2n)	yield of ^{130}I	[68–2]
^{142}Ce	(d,p)	yield of ^{143}Ce	[66–1] [69–12]
	(d,n)	yield of ^{143}Pr	[66–3] [69–12]
	(d,2n)	yield of ^{142}Pr	[66–3] [69–12]
	(d,α)	yield of ^{140}La	[66–3] [69–12]

ment was one of the pioneering work. The result of phase shift analysis is shown in Fig. 11–2.

The aim of the latter experiment was to obtain the excitation function of deuteron induced reactions. The energy of the deuteron from the Cyclotron is sufficient to observe the saturation behavior of deuteron induced reactions. Types of reactions investigated are listed above. The most significant conclusion of these investigations is, the deuteron induced reactions could be explained by modifying the Peaslee

Table XI–1. Grouping of states excited by j-forbidden stripping reaction. Protons from the (d,p) reaction leading to states in each group show angular distributions similar to each other. From [68–5].

Nucleus	Group	State	Configuration	Parity	Captured neutron state	$\sigma/\sigma_{s.p.}$ (%)
C^{13}	A	3.68, $3/2^-$ 7.53, $5/2^-$	$[(1p_{3/2}^{-1}\cdot 1p_{1/2})\cdot 1p_{1/2}]$	−	$1p_{1/2}$	44.0 26.1
	B	7.64, $3/2^+$ 9.90,	$[(1p_{3/2}^{-1}\cdot 1p_{1/2})\cdot 2s_{1/2}]$	+	$2s_{1/2}$	137.7 6.8
	C	6.86, $5/2^+$ 7.47, 9.50,	$[(1p_{3/2}^{-1}\cdot 1p_{1/2})\cdot 1d_{5/2}]$	+	$1d_{5/2}$	8.0 5.2 10.5
O^{17}	D	3.06, $1/2^-$ 3.85, $5/2^-$ 4.56, $3/2^-$ 6.87,	$[(1p_{1/2}^{-1}\cdot 1d_{5/2})\cdot 1d_{5/2}]$	−	$1d_{5/2}$	3.3 5.7 12.0 6.1
	E	5.22, 5.38, $3/2^-$ 5.94, $1/2^-$	$[(1p_{1/2}^{-1}\cdot 1d_{5/2})\cdot 2s_{1/2}]$	−	$2s_{1/2}$	36.2 15.2 17.4
Mg^{25}	F	1.611, $7/2^+$	$[Mg_{2+}^{24}+1d_{5/2}]$ $([1d_{5/2})_n^{-1}\cdot(1d_{5/2})_p^{3}\cdot(2s_{1/2})_p])$	+	$1d_{5/2}$	13.1

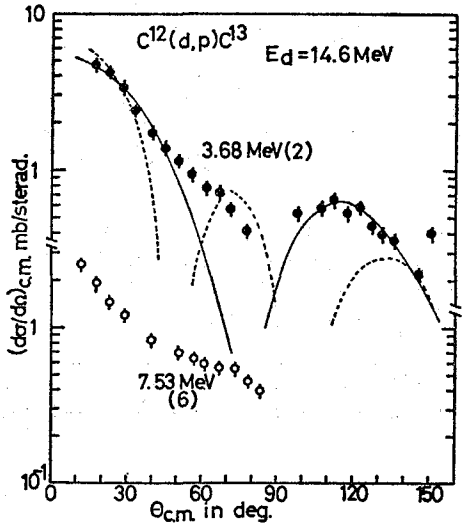

Fig. 11–1. Angular distributions of protons from $^{12}C(d,p)^{13}C$ reaction leading to the 3.63 MeV and 7.53 MeV states. E_d=14.6 MeV. The dashed line is the calculated curve on the basis of the knock out process. The solid line is calculated curve on the basis of two step process. Both lines are normalized properly. From [68–5].

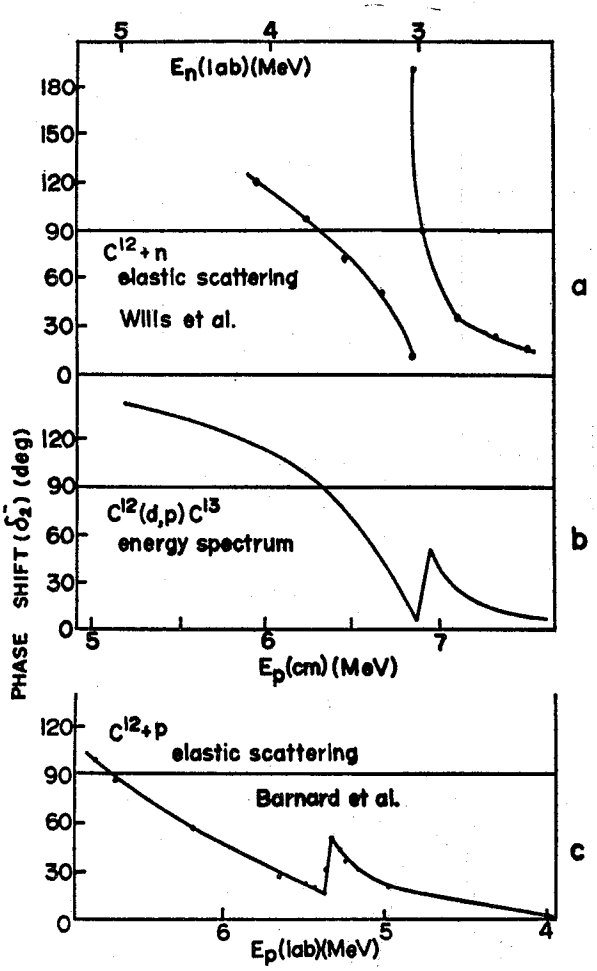

Fig. 11–2. Comparison of phase shifts obtained by elastic scattering and final state interaction. (a). Phase shifts δ_2^- of the neutron-^{12}C scattering. Data of Wills *et al.* (b). Approximate phase shifts δ_2^- obtained from the proton spectrum of the ^{12}C(d.p)^{13}C reaction. The phase shifts contain uncertainty of $\pm 5°$ and are normalized at $E_p^{cm} = 6.45$ MeV. (c). Phase shift δ_2^- of the proton-^{12}C scattering obtained by Barnard *et al.* From [70–3].

theory aided by the statistical theory. Figure 11–3 shows the fit of statistical theory to the deuteron induced reactions on ^{142}Ce. The fit is not good except for (d,2n) reaction and therefore the reactions could not be explained by the compound process only. Figure 11–4 shows the theoretical fit of modified Peaslee theory together with the satistical theory. The fit is satisfactory. Peaslee theory stands for the direct stripping process and it assumes that only a neutron or a proton of deuteron is inside

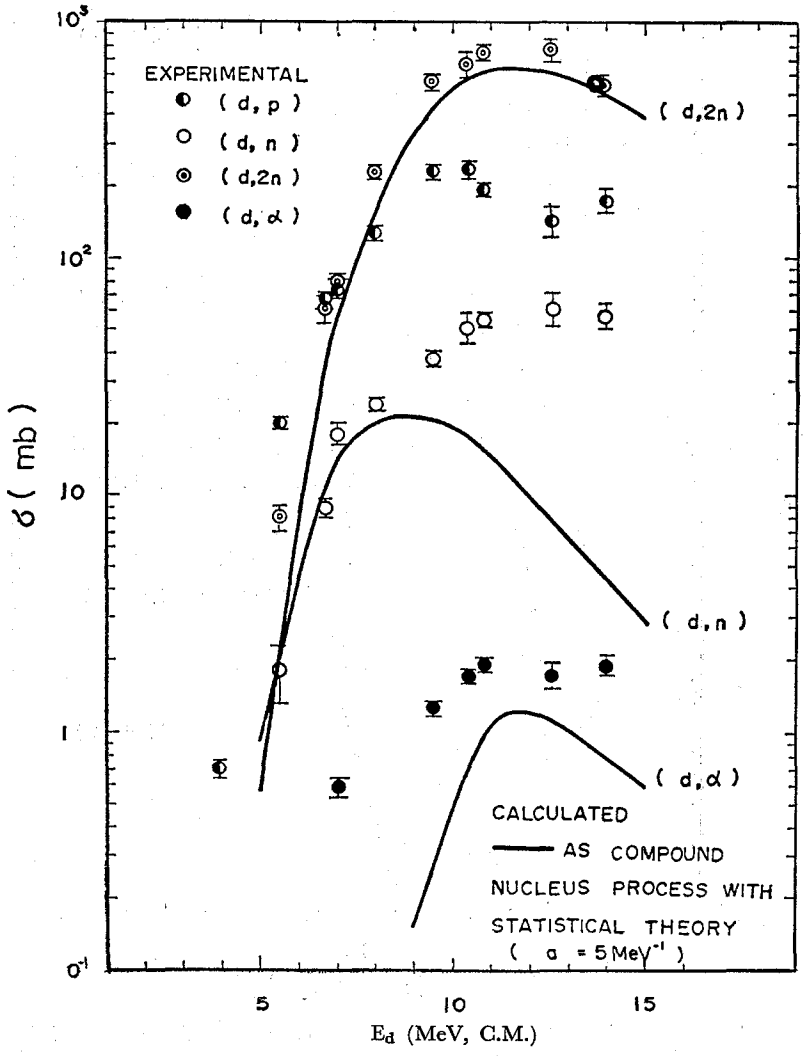

Fig. 11–3. Comparison between the cross sections calculated from the compound process with the statistical theory and the experimental ones. Target material is ^{142}Ce. From [69–12].

the interaction range of the target nucleus. Otozai *et al.* [68–2] assumed that there is a fairly large probability of entire absorption of deuterons by the target nucleus. They expressed their assumption by introducing a new parameter, entire absorption radius, and got a satisfactory fit to the experiment. This result means that the deuteron is not so fragil as commonly expected. A naive question, at where the deuteron breaks into a proton and a neutron, arises from these experiments.

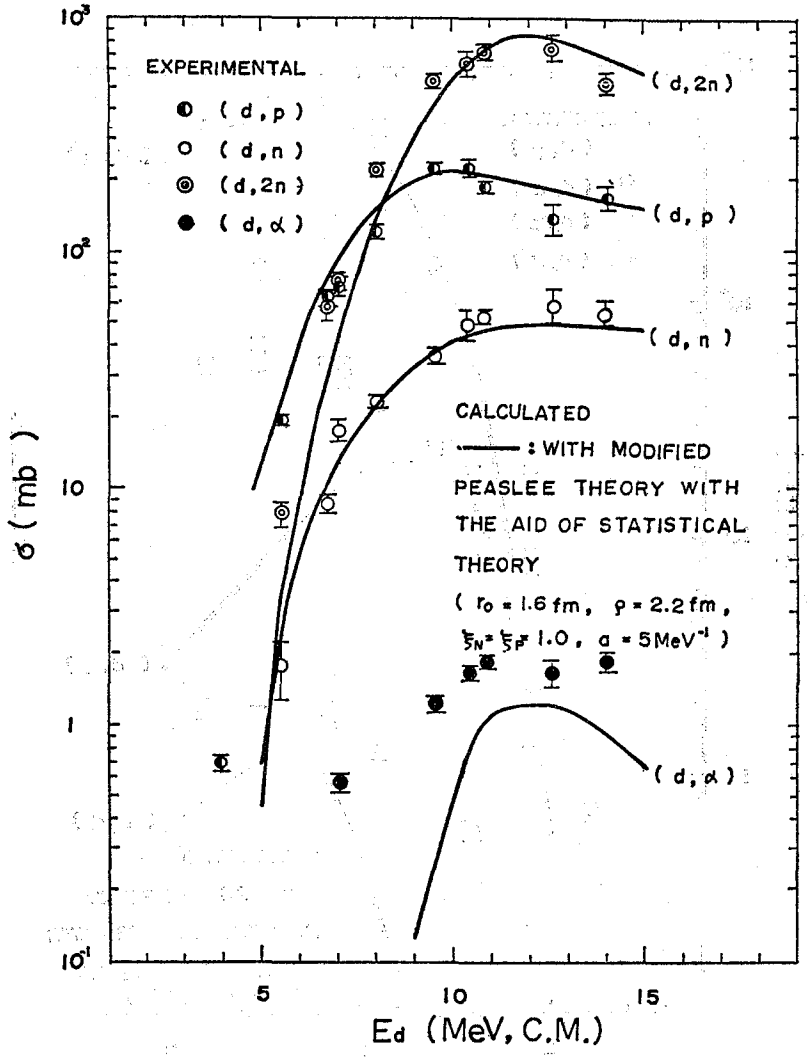

Fig. 11–4. Best fitting of the modified Peaslee theory with the aid of the statistical theory to the experimental cross sections. Experimental data are the same in Fig. 11–3. From [69–12].

Reactions investigated	Reference
^{9}B(p, p) ^{9}Be*(1.67)	[74–2]
^{9}Be(p, p′)^{9}Be	[74–7]
^{9}Be(p, d)^{8}Be	[74–7]
^{9}Be(p, α)^{6}Li	[74–7]
^{11}B(α, ^{7}Li)^{8}Be	[68–9]
^{24}Mg(α, d)	[66–7]
^{28}Si(α, d)	[66–7]
^{32}S(α, d)	[66–7]
^{40}Ca(α, d)	[66–7]
^{51}V(α, t)	[68–10]
^{55}Mn(α, t)	[68–10]

XII. REARRANGEMENT REACTION AND NUCLEAR STRUCTURE

The title above mentioned means the nuclear reactions by protons and alpha particles other than the elastic and inelastic scattering and the aim of the reaction researches are laid prominently on the structure of the nucleus.

Types of reactions and references are listed up in the table of p. 101. These reactions were investigated by different group members and from different motivations, so that the consistency among these experiments does not exist.

Proton induced reactions on ^{9}Be was studied to clarify the level structure of ^{10}B. The aim of the authors was to assertain the existense of singlet deuteron coupled to the ^{8}Be core. Their expectation was not satisfied by this experiment but they found some new levels of ^{10}B and also found that some levels appear in only a specified reaction channel. Van de Graaff accelerator of the Department of Physics were used to obtain the excitation functions of various reaction channels listed. Newly found levels and their structures are listed in Table XII–1. Among these levels, the 11.2 MeV excited state was studied with special care and the structure of this level was suggested to be [2 nucleons $(2s+1d)+^{8}$Be $(0^{+}+2^{+})$]. Therefore, this level has essentially a three body structure, n+p+excited ^{8}Be core.

Table XII–1. Energy levels of ^{10}B in the excitation energy from 10.2 MeV to 12.0 MeV. For references, see [74–7].

present work					previous works[a]	
E_p (MeV)	E_x (^{10}B) (MeV)	Γ (keV)	J^{π}, T	decay channels	Γ (keV)	decay channels
4.5	10.6	1 MeV		p_0		
4.5	10.6	200	, 0	p_0, α_0		
4.7	10.8	300	2^{+}, 1	p_0, p_2, α_2, (α_1)	500	n, α_2
5.1	11.2	300		p_1		
5.5	11.5	500	isospin impure	α_1, α_2	270±50	

(a) See References 4, 7, and 8.

^{11}B(α,^{7}Li)^{8}Be reaction was investigated as an example of heavy ion reactions. The residual nucleus, ^{8}Be, is unstable and breaks into two alpha particles, therefore, this reaction is a kind of three body reactions. However, the result is very interesting aside from the view of the three body reaction. First, the emitted ^{7}Li has two states, that is, ^{7}Li ground state and ^{7}Li in its first excited state are emitted simultaneously leaving ^{8}Be in its ground state. The angular distributions of ^{7}Li(g′nd) and ^{7}Li(1st, 0.478 MeV) are shown in Fig. 12–1. This reaction is an inverse reaction of ^{8}Be (^{7}Li,α)^{11}B. Therefore, one can expect if ^{8}Be is bombarded by ^{7}Li ions, different types of reactions can occur in which the incident ^{7}Li particle is excited or not. As seen from Fig. 12–1, the angular distribution of ^{7}Li(g′nd) differs so much from that of ^{7}Li(1st). These facts suggest that the mechanism of triton pickup by an alpha particle from ^{11}B is complicated and interferences of both types of reactions might affect the angular distributions. On the other hand, this reaction clarifies in the sense

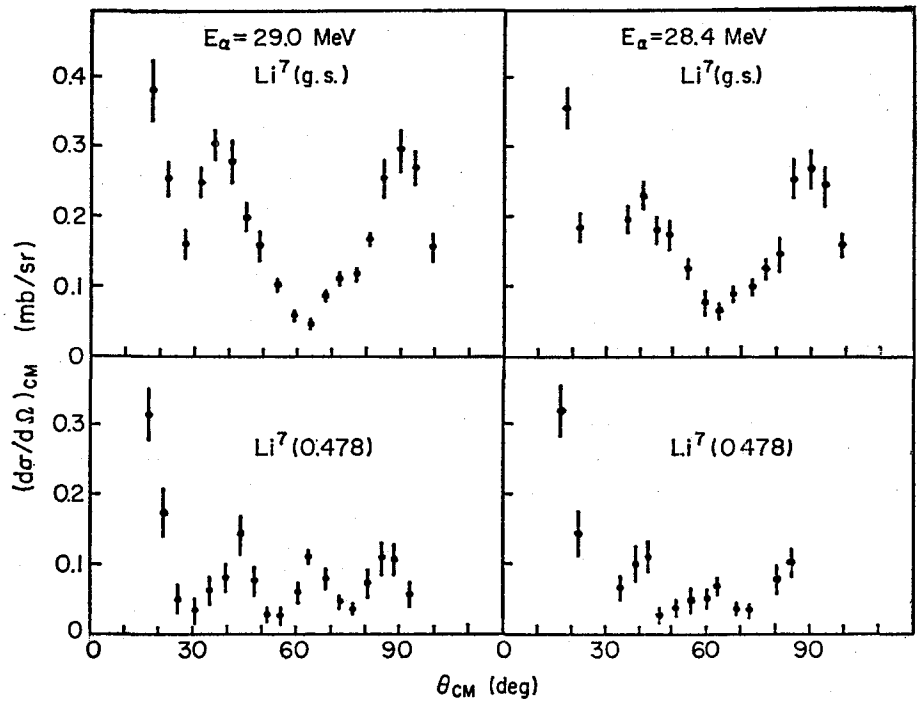

Fig. 12-1. Angular distributions of ^{7}Li(g.s.) and ^{7}Li(0.478 MeV) from the reaction ^{11}B(α, ^{7}Li)^{8}Be(g.s.) at 29.0 MeV and 28.4 MeV. From [68-9].

Table XII-2. Comparison of ^{30}P Levels Observed by the (α,d) Reaction with Those Previously Reported For references, see [66-7].

Levels observed (MeV)	Previously reported levels (MeV)	J^π	T	Dominant configuration	Intensity[c]
0	0	1^+	0	(s1/2d3/2)b	0.87 mb
	0.684	0^+	1	(s1/2)^{2}b	
0.70	0.705	1^+	0	(s1/2)^{2}b	0.64 mb
1.45	1.451	2^+	0		0.37 mb
1.97	1.972	3^+	0		0.77 mb
	2.538	(3^+	0)	(d3/2)^{2}b	
2.6	2.723	2^+	0		1.26 mg
	2.839				
	2.937	2^+	1		
	3.018	1^+			
4.17±0.05		(5^-)	0	(d3/2f7/2)	1.91 mb
4.90					strong
5.70±0.07					fairly strong
7.11	7.03[a]	7^+	0	(f7/2)^2	1.57 mb
8.0 ±0.1					fairly strong
9.0					fairly strong
9.25		(3^+)	0	(p3/2)^2	strong

a ref. 18). b ref. 20). c Range of integration: 15 to 100 deg (C.M.). d ref. 10).

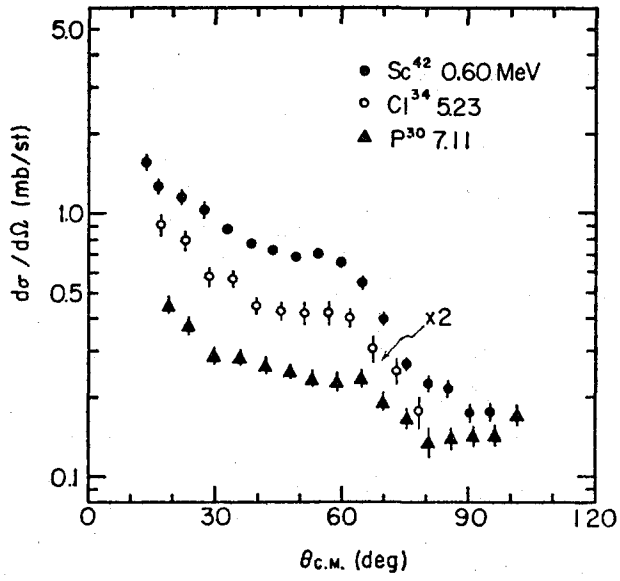

Fig. 12–2. Angular distributions of deuterons leading to the levels at 7.11, 5.23, and 0.60 MeV of ^{30}P, ^{34}Cl, and ^{42}Sc respectively. These levels are considered to arise from the $(f7/2)^27$ configuration. From [66–7].

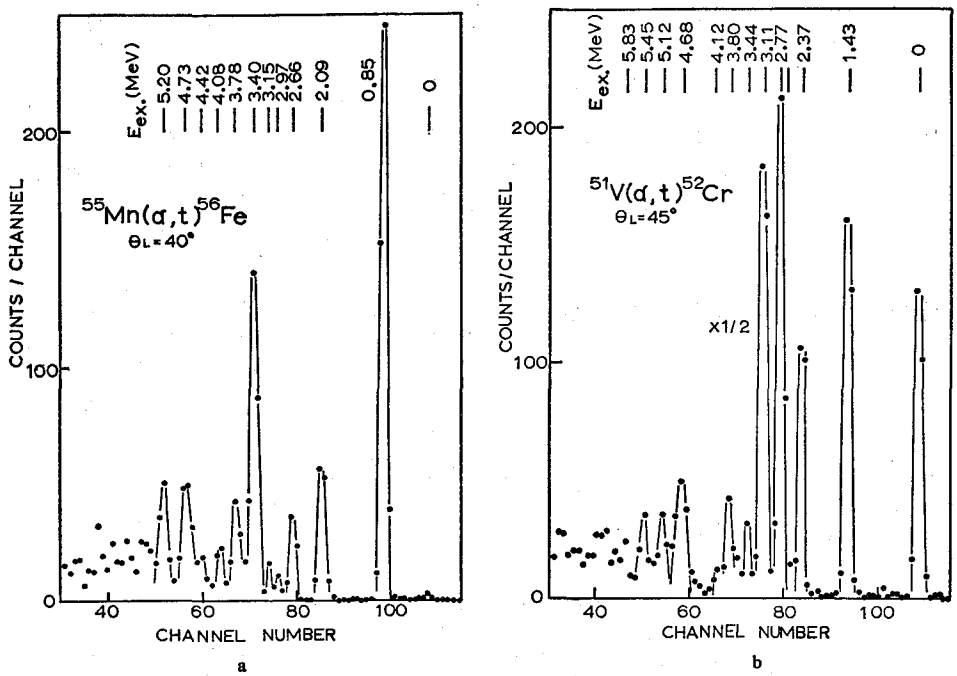

Fig. 12–3. Pulse-height spectra of tritons from (α, t) reaction on (a) ^{51}V and (b) ^{55}Mn. The levels are identified by their excitation energies. From [68–10].

that the ground and first exicted state of ^{7}Li consist of triton and an alpha particle but their coupling scheme is different with each other.

The (α,d) reaction in ^{24}Mg, ^{28}Si, ^{32}S, and ^{40}Ca was investigated to find the two particle states in the residual nuclei. The target nuclei are all even-even nucleus, therefore, one can expect to excite the two nucleon states coupled to the even-even nuclear core by this reaction. Since the energy of alpha particles is 29 MeV, maximum transfer angular momentum is 4 to 5$\hbar$ and a nucleon can be captured in 2s1/2, 1d3/2, and 1f7/2 states. The result for the ^{28}Si is shown in Table XII–2. Figure 12–2 shows the angular distribution of deuteron leavings the residual nuclei in the same $(f7/2)^{2}7$ configurations. The similarity between these angular distributions are obvious.

The (α,t) reactions in ^{51}V and ^{55}Mn were investigated to enclothe the $(1f7/2)^{n}$ proton states in ^{52}Cr and ^{56}Fe. Protons, deuterons and tritons emitted were indentified by the aid of two dimentional representation of counter telescope. Energy spectra of tritons are shown in Fig. 12–3. They fitted the angular distributions of tritons with INS-DWBA-2 code and then obtained the spectroscopic factors for $(1f7/2)^{n-1}\rightarrow(1f7/2)^{n}$ transitions with the aid of seniority scheme. Some of the results are listed in Table XII–3. In the original paper, they compared the results obtained from (α,t) reactions with those from (^{3}He, d) reactions. The transition strengths obtained from (α,t) reactions are somewhat smaller than those from (^{3}He, d).

Table XII–3. Spectroscopic Factors ($1f7/2$) Orbit Obtained from the (a, t) Reaction and Comparison with the Theoretical Values. From [68–10].

Target nucleus	Residual nucleus	Theory[a]						Experiment[b]			
		n	ν_1	J_1^{π}	ν	J^{π}	spectroscopic factor	J^{π}	spectroscopic factor		excitation energy (MeV)
^{51}V	^{52}Cr	4	1	$7/2^{-}$	0	0^{+}	4.0	0^{+}	4.0[c]		0.0
					2	2^{+}	1.33	2^{+}	1.09		1.43
					2	4^{+}	1.33	4^{+}	0.47	1.19	2.37
								4^{+}	0.72		2.77
					2	6^{+}	1.33	6^{+}	1.06		3.11
^{55}Mn	^{56}Fe	6	3	$5/2^{-}$	0	0^{+}	0.0	0^{+}	0.06		0.0
					2	2^{+}	2.20	2^{+}	1.74	1.91	0.85
								2^{+}	0.17		2.66
					2	4^{+}	0.12	4^{+}	0.24		2.06
					2	6^{+}	0.45	(6^{+})	0.42		3.40
^{59}Co	^{60}Ni	8	1	$7/2^{-}$	0	0^{+}	8.0	0^{+}	5.20		0.0

a) Ref. [27]. b) Table 2. c) Normalized.

XIII. THREE BODY REACTIONS

When a reaction between two particles results into three particles, this type of reaction is called three body reaction or three particle reaction. In our laboratory, a series of investigations to find the alpha clustering in the nucleus, and other series of investigations to find final state interaction among final two particles, were com-

Reaction	Detected Particle	Reference
$d+p \rightarrow p+p+n$	p, p	[72–2]
$d+d \rightarrow p+d+n$	p, d	[68–4]
$d+\alpha \rightarrow p+n+\alpha$	p, α	[67–9] [68–4]
$^{6}Li+\alpha \rightarrow \alpha+\alpha+d$	α, α, d	[68–3]
$^{6}Li+\alpha \rightarrow d+\alpha+\alpha$	d	[74–8]
$^{7}Li+\alpha \rightarrow \alpha+\alpha+t$	α, α, t	[68–3]
$^{7}Li+\alpha \rightarrow t+\alpha+\alpha$	t	[74–8]
$^{9}Be+p \rightarrow p+\alpha+^{5}He$	α, p	[67–11] [67–3] [69–1]
$^{9}Be+\alpha \rightarrow \alpha+\alpha+^{5}He$	α, α	[68–1]
$^{11}B+\alpha \rightarrow \alpha+n+^{7}Li$	α, α	[69–16]
$^{11}B+p \rightarrow p+^{8}Be \rightarrow \alpha+\alpha+\alpha$	α, α	[74–9]
$^{12}C+p \rightarrow p+\alpha+^{8}Be$	p, α	[67–11] [67–3]
$^{12}C+p \rightarrow p+\alpha+\alpha+\alpha$	p, α	[72–3]
$^{12}C+\alpha \rightarrow \alpha+\alpha+^{8}Be$	α, α	[68–1] [67–3]
$^{16}O+\alpha \rightarrow \alpha+\alpha+^{12}C$	α, α	[67–11]
$^{20}Ne+\alpha \rightarrow \alpha+\alpha+^{16}O$	α, α	[67–11]

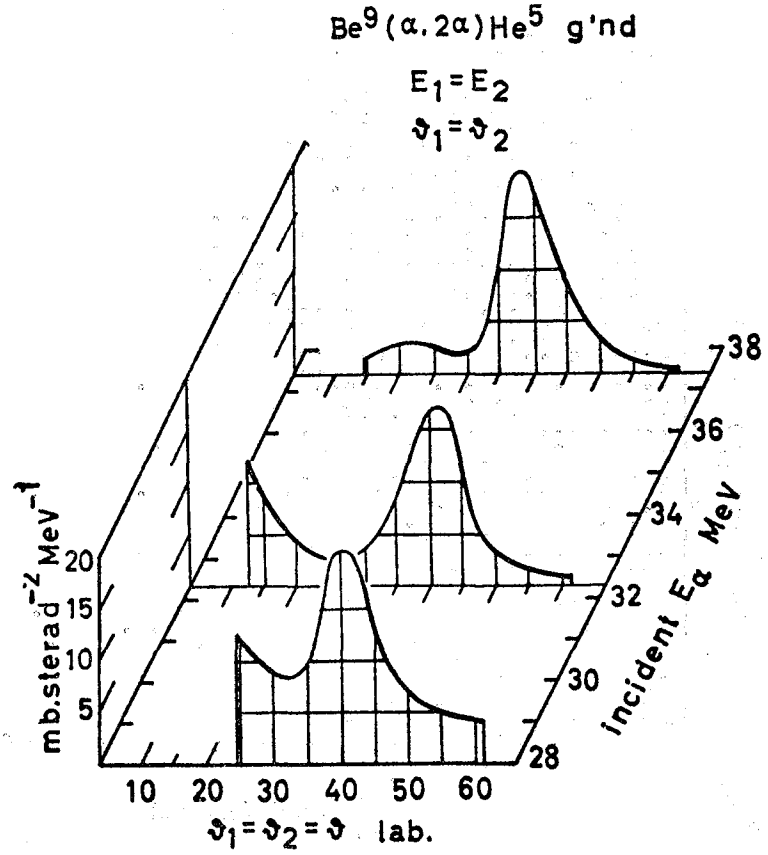

Fig. 13–1. Angular correlation distribution between two alpha particles with the same energy and emitted to the symmetrical direction around the beam. The reaction is $^{9}Be(\alpha, 2\alpha)^{5}He$(g'nd). From [68–1].

bined and three body reaction was continuously investigated since the end of the past decade. To promote this type of investigation, a scattering chamber of special structure was constructed [69–11]. By the use of this chamber and an alpha beam of the Facility and sometimes a proton beam and an alpha beam of the Institute for Nuclear Study, University of Tokyo, three body reactions of various types listed in the preceding Table were investigated. Target nuclei are limited within light nuclei, because the emerging particles have too low energy to be detected when heavy elements were used as targets.

Quasi free α-α scattering experiment in ^{9}Be had established the alpha cluster existence in ^{9}Be and has been extended to investigate the existence of alpha clusters in heavier nuclei, that is, in ^{11}B, ^{12}C, ^{16}O, and ^{20}Ne. Conclusions from this series of

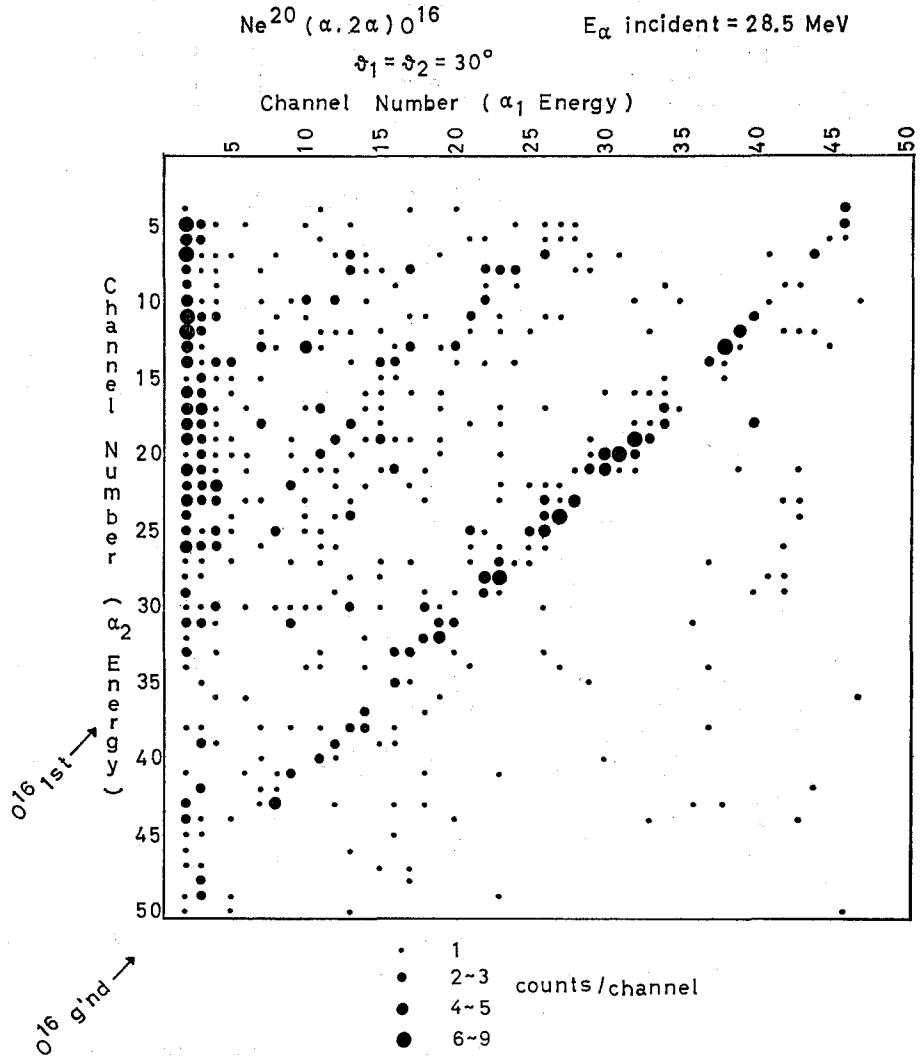

Fig. 13–2. Energy correlation between two alpha particles from the ^{20}Ne(α, 2α)^{16}O reaction. Arrows show kinematical loci of ^{16}O(g'nd) and ^{16}O(1st). Unpublished.

experiments are, when the nucleus becomes heavier, the existence of alpha clusters becomes vague and quasi free $\alpha-\alpha$ scattering becomes rarer, and alpha particle decay from the target nucleus (of course it is excited) becomes dominant. Especially, the investigation of $(\alpha,2\alpha)$ reaction in ^{20}Ne clearly showed the levels of ^{20}Ne composed of an alpha particle and a ^{16}O nucleus. Thus the investigation of $\alpha-\alpha$ quasi free scattering results in studies of sequential decay problem and cluster structure of excited states of target nucleus. Figure 13–1 shows the angular correlations of two alpha particles from the ^{9}Be$(\alpha,2\alpha)^{5}$He reaction. The energy of the incident alpha particle varies from 28 MeV to 37 MeV. In this figure, quasi-free scattering between the incident alpha particle and intranucleus alpha cluster is clearly seen. Contrary to this figure is the next Fig. 13–2. This figure shows the energy correlation of two alpha particles from the ^{20}Ne$(\alpha,2\alpha)^{16}$O reaction. As seen from the figure, summed energy spectra lie on lines corresponding to the ground and first excited state of ^{16}O, and moreover, the dense parts of the two dimensional spectra are localized and separated with each other. This fact means that one of two alpha particles is a decay product from ^{20}Ne in alpha emitting excited states. Thus the ^{20}Ne$(\alpha,2\alpha)^{16}$O reaction shows clearly the feature of sequencial decay. The course of investigations was changed when we became aware of the importance of sequential decay process, and a new field of research was opened, that is, the investigation of the cluster structure of the excited states of the nucleus by the method of decay correlation measurements. The structure of the excited states of ^{6}Li, ^{7}Li, ^{11}B, and ^{12}C were investigated by this method. Figure 13–3 shows the alpha-triton azimuthal angular correlation distribution for the 4.63 MeV state of ^{7}Li. In the experiment, an alpha counter was fixed and a triton counter was moved around the recoil axis of ^{7}Li(4.63 MeV) with a constant polar angle of 30°. From this and other results

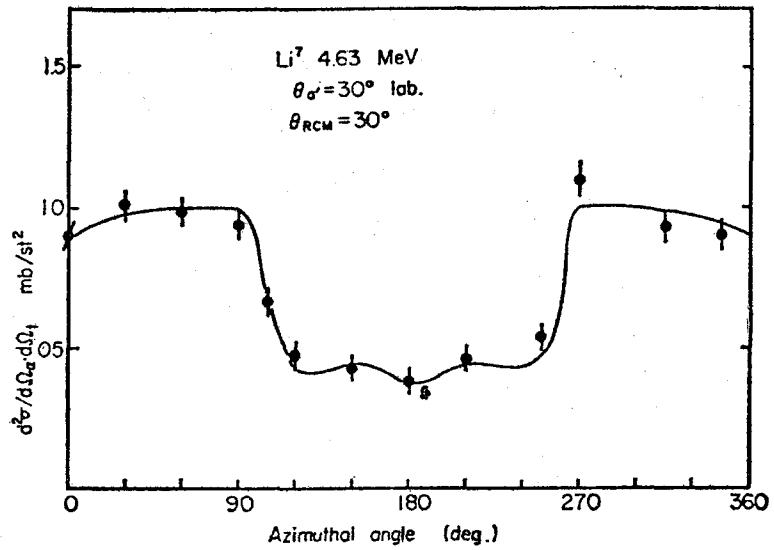

Fig. 13–3. The alpha-triton azimuthal angular correlation distribution for the 4.63 MeV state of ^{7}Li. The triton counter was moved around the recoil axis with a constant polar angle of 30° in the recoil center of mass system. From [68–3].

obtained, the spin parity of the 4.63 MeV state of ^{7}Li was assigned to be $7/2^-$.

Final state interactions observed in our laboratory are those of p-n, p-α, n-α, and α-α. Figure 13–4 shows the proton-alpha coincidence spectra from the D(α,pα)n reaction. As shown in the figure, broad peaks are observed on the kinematical locus of ^{5}He(g'nd). These peaks are due to the final state interaction between a neutron and an alpha particle to form the ^{5}He(g'nd). Proton-alpha final state interaction leading to the ground state of ^{5}Li was observed also in this experiment. It is interesting that the width of these particle unstable state obtained by the three body reaction coincides with that obtained from the scattering experiment.

Final state interaction was applied also to investigate the p-n singlet state. Matsuki *et al.* carried out the experiment of D(p,2p)n reaction and searched the deuteron singlet state. The result was negative. However, quite recently, Fujiwara *et al.* found an excited state of ^{3}He composed of a proton and a singlet deuteron. Other final state interactions are mainly concerned with alpha-alpha resonances. Kakigi *et al.* investigated the $B^{11}+p\rightarrow\alpha+\alpha+\alpha$ reaction and assigned the spin-parity of 2.9 MeV excited state of ^{8}Be to be 2^- by observing the peak of alpha particles corresponding this state [74–9].

A peculiar peak which does not correspond to the state of ^{8}Be was also found by the investigation of ^{7}Li(α,t)$\alpha\alpha$ and ^{6}Li(α,d)$\alpha\alpha$ reactions. Figure 13–5 shows the energy spectra of tritons from ^{7}Li(α,t)$\alpha\alpha$ reaction. Broad peaks in the left hand side of the spectra have no corresponding ^{8}Be state. Matsuki *et al.* concluded that these peaks of tritons come from the break up of target nucleus when it is excited by the incident particle. This fact correlates with ^{11}B(α, ^{7}Li)^{8}Be reaction [68–9].

It is also an interesting problem if the final three particles are at the same time in the range of interaction or not. If two among three particles are in resonance state, this resonance state should be modified by the existence of remaining third particle. If two sets of two particles among three particles are in resonance simultaneously, some constructive or destructive effect is expected. In a series of experiments in our laboratory, these two body resonance overlapping phenomena were

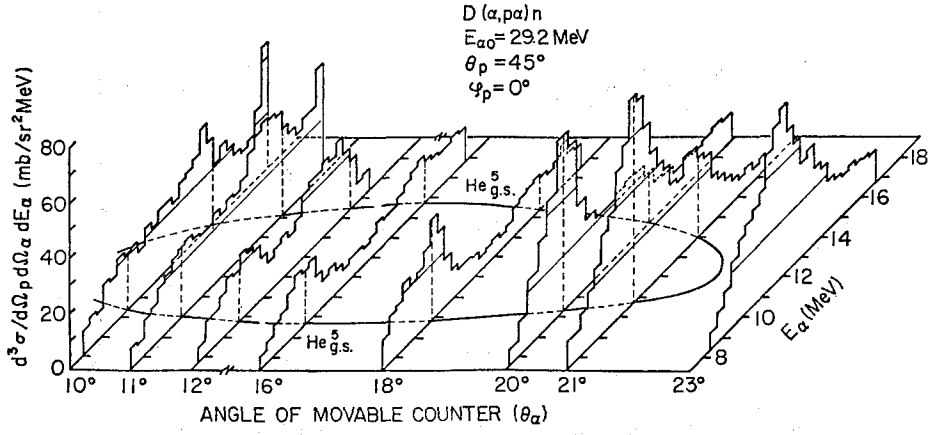

Fig. 13–4. Coincidence energy spectra of alpha particles from the $D(\alpha, p\alpha)n$ reaction in a three dimensional form. The proton counter is fixed at 45° of θ_p and 0° of φ_p. The locus of ^{5}He(g.s.) is also shown. From [68–4].

observed. A typical investigation is that of Fujiwara [69–16]. He observed the $^{11}B+\alpha\rightarrow\alpha+\alpha+^{7}Li$ reaction and concluded this reaction occurs following two ways. One is $^{11}B+\alpha\rightarrow\alpha+^{11}B^{*}\rightarrow\alpha+\alpha+^{7}Li$ and the other is $^{11}B+\alpha\rightarrow^{8}Be+^{7}Li\rightarrow\alpha+\alpha+^{7}Li$. Fujiwara found that in this reaction both way of reaction occur simultaneously and two alpha particles and a ^{7}Li exist in some time interval in the range of interaction.

Conclusions hitherto obtained in our laboratory indicate that, three body reaction should not be interpreted by too simple models such as spectator model, quasi-free scattering model, direct breakup model, final state interaction model

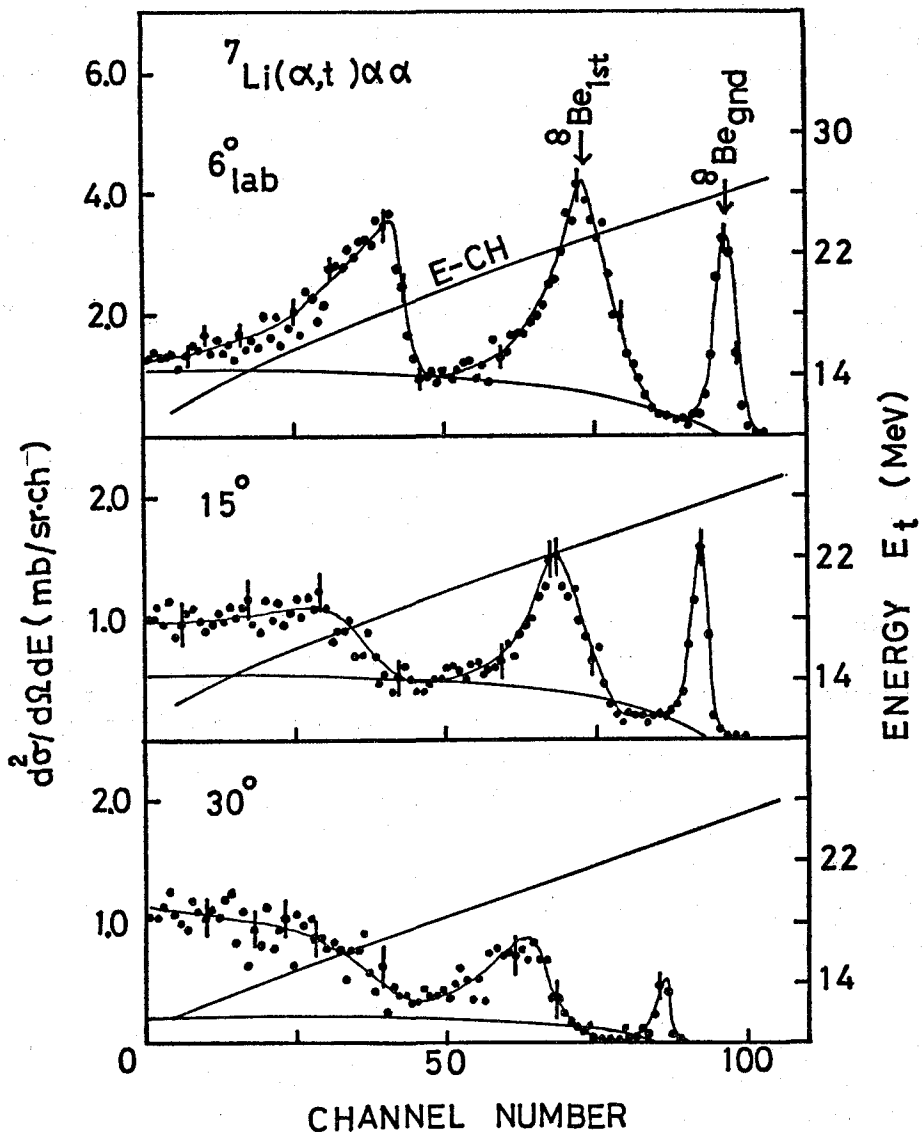

Fig. 13–5. Energy spectra of tritons at 6°, 15°, and 30° (lab) from the $^{7}Li+\alpha$ reaction with 29.4 MeV alpha particles. Typical error bars are shown. The curve labelled E-CH gives the relation between particle energy and channel number. The smooth curves are the prediction of the phase space factor. From [74–8].

and sequencial decay process model. The matter is not so simple and these processes occur simultaneously in the three body reactions at low energies.

XIV. INTERMEDIATE ENERGY NUCLEAR PHYSICS

The title "Intermediate Energy Nuclear Physics" means the nuclear structure and reaction studies by using more than 100 MeV and less than a few GeV protons or electrons. This branch of research was developed intensively since 1966 in U.S.A. and in Europe. In our laboratory, this intermediate energy nuclear physics became an object of attension in the early 1962, when the future program to promote the nuclear and particle physics in Japan was discussed among researchers. In those days, particle physicists were eager to build accelerators of higher and higher energy. Synchro-cyclotrons of a few hundred MeV were built and were used to verify the nature of pions and then were shut down one after another. The nuclear structure studies by these synchro-cyclotrons were scarce and were skipped. However, as a consequence of research works in our laboratory, nuclear physics at intermediate or high energy seemed an inevitable and natural development of nuclear physics at low energy. One reason, for example, is that, at low energy, the particle energy produced by three body reactions is often two low to be detected and is embodied in the noise level, therefore, higher energy machine was hoped.

Two different approaches had been followed in our laboratory to develop the intermediate energy nuclear physics. One way was to do research works in this region by using the existing machine in collaboration with other laboratories. The other way was to promote the organization in Japan to prepare oneself when the accelerators in the National Laboratory for High Energy Physics become feasible.

First, we introduce the results obtained in this decade following the former approach. One item is the study of quasi-free scattering between high energy electrons and protons in the nucleus. Since 1970, in collaboration with members of University of Tokyo, this study was started [72–5], [73–2], [74–16], and [76–3]. They used as projectiles the 700 MeV electron beam extracted from the electron synchrotron of the Institute for Nuclear Study, University of Tokyo. The method of electron beam extraction is described in section III of this article. Target nuclei they studied are, ^{6}Li, ^{7}Li, ^{9}Be, ^{12}C, ^{27}Al, ^{40}Ca, and ^{51}V. Figure 14–1 shows the experimental arrangement. Electrons scattered from protons in the nucleus were detected by a momentum analyzing magnet plus scintillation counter plus gas Cherenkov counter system. Protons ejected from the nucleus were detected by a set of range spark chambers. Detection angles were decided so as to detect quasi-free electron proton scattering. The aim of this experiment was to determine the separation energies of 1s and 1p state protons and momentum distributions of these protons simultaneously. In Fig. 14–2 is shown the separation energies of 1s and 1p state protons as functions of mass number. These results give more reliable values than those obtained by (p,2p) quasi free scattering experiments.

Further, they analyzed the data with distorted wave impulse approximation and

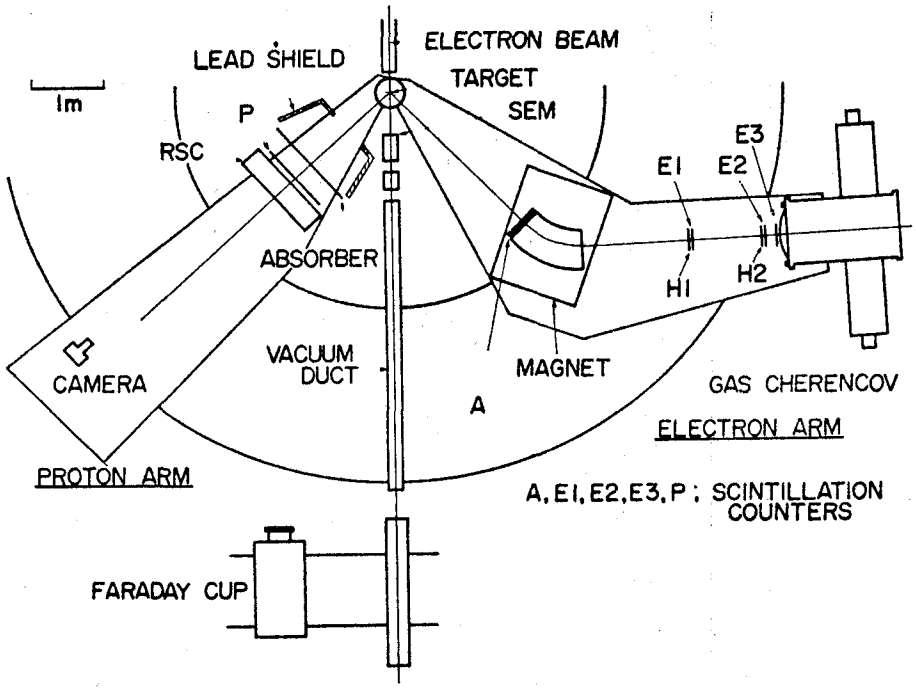

Fig. 14–1. Experimental arrangement to detect the quasi-free electron proton scattering. Target nuclei are, ^{6}Li, ^{7}Li, ^{9}Be, ^{12}C, ^{27}Al, ^{40}Ca, and ^{51}V.

obtained the momentum distribution of protons. As an example, in Fig. 14–3 is shown the experimental and calculated results of momentum distribution of 1s protons in ^{12}C. From the theoretical analyses, they concluded that for nuclei heavier than ^{12}C, the single particle model gives good fit, but for ^{6}Li and ^{7}Li, cluster structure of these nuclei strongly affect the momentum distribution of 1s and 1p protons.

Other items in this field were carried out in collaboration with Orsay Institute for Nuclear Physics, University of South Paris. By using 156 MeV proton beam from the synchrocyclotron, proton elastic scattering from ^{4}He, ^{4}He(p,2p)^{3}H, ^{4}He(p, pd)^{2}H, ^{3}He(p,pd)H, ^{3}He(p,2p)^{2}H, and ^{3}He(p,pn) reactions were investigated [75–1], [75–2], and [75–3]. Elastic scattering of protons from ^{4}He was studied to test the interaction mechanism between protons and ^{4}He. Optical model analysis and Glauber approximation were made and informations about the nuclear exchange force were obtained. In the ^{4}He+p reaction, single particle nature and p-n short range correlation in ^{4}He were investigated. In the investigation of breakup of ^{3}He by 156 MeV protons, p-p quasi-free scattering and p-n quasi-free scattering were compared. Further, p-d and p-p-n final state interactions were investigated to obtain informations about the excited states of ^{3}He. Figure 13–4 shows the energy spectra of protons in coincidence with protons or neutrons from the (p,2p) or (p,pn) reaction respectively. As seen from this figure, no essential difference exists between (p,2p) and (p,pn) reaction. Spectator model is useful in these reactions because the spectra could be resembled with simple plane wave impulse approximation. In Fig. 14–5 is shown the energy spectrum of protons from the (p,pd) reaction. Aside from

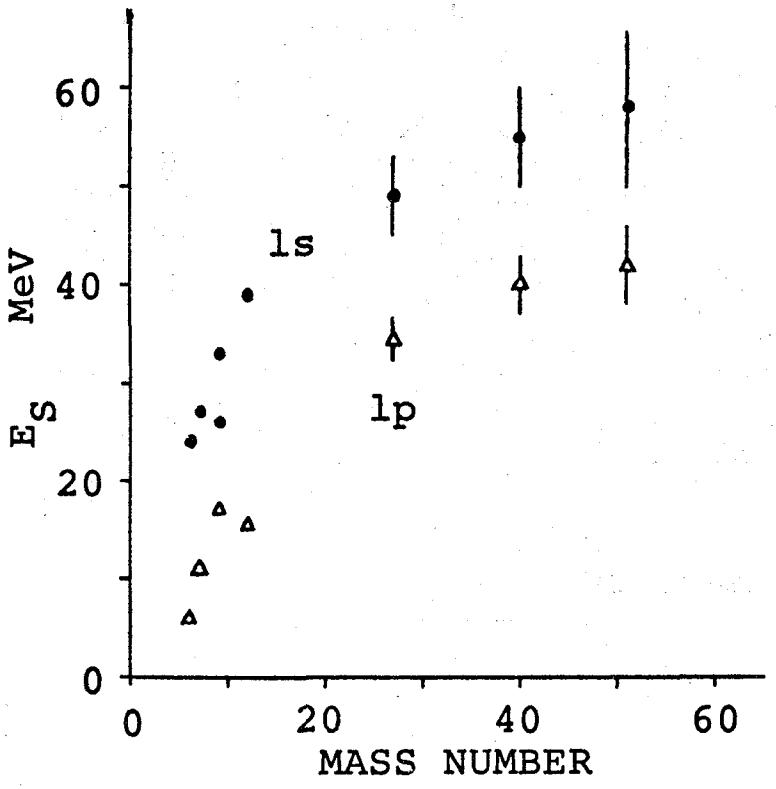

Fig. 14–2. The separation energy of 1s and 1p state protons as a function of the mass number. From [72–5].

the quasi-free p-d scattering peak, small peak is observed in the left-hand side due to the p-d or p-d final state interaction. This peak seems to show the excited state of ^{3}He.

Second, we introduce the results obtained in this decade following the latter approach. This way of approach consists of design studies of instrumentations to use the beam from the accelerators of the National Laboratory for High Energy Physics, the holding of workshops on the nuclear physics which will be investigated using the beam, and the planning of proposals to the National Laboratory, [69–15], [70–1], [70–4], [70–5], [73–1], [74–1], and [74–14]. These works were aided financially partly by the National Laboratory and partly by the Grant in Aid of Ministry of Education. The accelerator of the National Laboratory for High Energy Physics consists of four stage accelerators; pre-injector, linear accelerator, booster synchrotron and main accelerating synchrotron. The booster synchrotron can offer surplus proton beam of 500 MeV. Main synchrotron produces proton beam of 8 to 12 GeV. In the intermediate energy nuclear physics, main concern was with the utilization of 500 MeV proton beam and of kaons, pions, muons and anti-protons produced by the 8 to 12 GeV protons. Further, nuclear fragmentations, spallations and fissions were discussed by nuclear chemists and cosmic ray physicists. Totally, about 140 participants attended the meetings on physics and/or instrumentations.

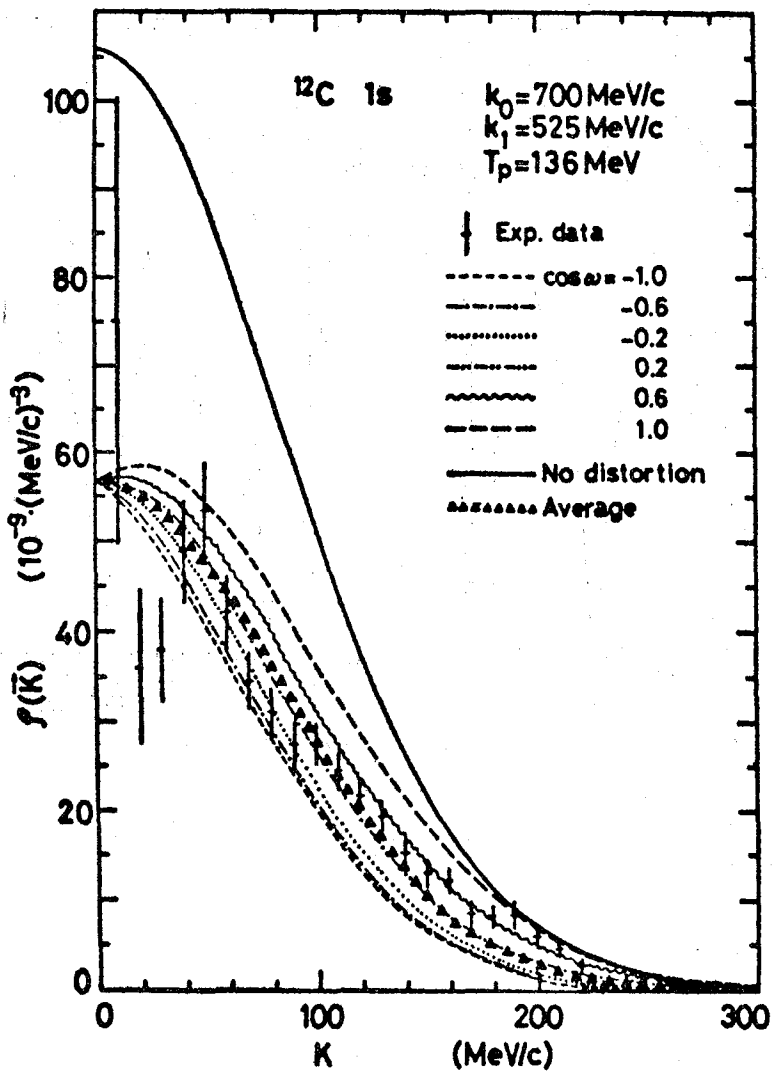

Fig. 14–3. Distorted momentum distribution of the 1s state protons in ^{12}C as a function of K. For the meaning of cos ω, see [76–3].

Physics items discussed were:

1) construction of low momentum enriched beam channel of kaons, pions, and anti-protons.
2) radiative capture of pions by the nucleus.
3) muon capure by the nucleus and hyperfine structure of mu mesic atoms.
4) kaon capture by the nucleus and neutron proton distribution in the nucleus.
5) kaon capture by the nucleus and the spectroscopy of hypernucleus.
6) mesic atoms formed by strongly deformed nuclei.
7) magnetic moment of sigma particle in a nucleus.
8) neutron emission from the nucleus induced by muon capture.

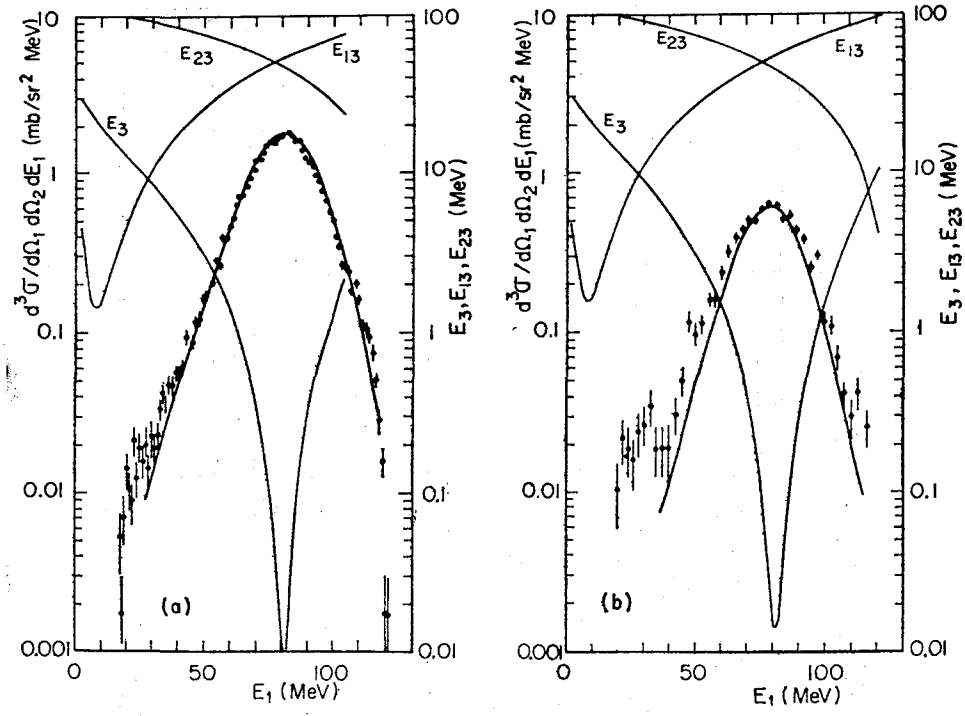

Fig. 14–4. (a) The $d^3\sigma/d\Omega_1\, d\Omega_2\, dE$, spectrum for $^3\mathrm{He}(p, 2p)d$ and ⇩ at $\theta_{p1}=40°$ and $\theta_{p2}=-44°$. (b) The same spectrum for $^3\mathrm{He}(p, pn)2p$. Error bars are statistical. The solid curve E_3 indicates the kinematic energy (lab) of the recoil deuteron or the two nucleon system, and E_{13}, E_{23} indicate the relative energies between the proton detected by the first detector (or the second nucleon by the second detector) and the spectator deuteron or a two nucleon system. The solid lines along the experimental points represent the $d^3\sigma$ calculated with PWIA. From [75–3].

9) polarization of the nucleus induced by pion capture.
10) isobaric analogue states formed by electrons, pions, and muons.
11) pion charge exchange reaction.
12) inner deuteron wave function estimation by the pion plus deuteron reaction.
13) anti-proton neutron bound state.
14) proton-proton scattering and measurement of higher order parameters.
15) neutron-proton, proton-proton, antiproton-proton scattering and Regge pole model.
16) comparison between bound and scattering state of kaon-nucleus system.
17) slope parameter of kaon and pion scattering from the nucleus and the relation to the neutron and proton distribution in the nucleus.
18) transition charge density of the nucleus determined by inelastic scattering of pions and electrons.
19) three body forces between pi-lambda-nucleon, kaon-xi-nucleon and kaon-sigma–sigma systems.
20) the systematics of spallations, fragmentions and fissions of heavy nuclei induced by high energy protons.

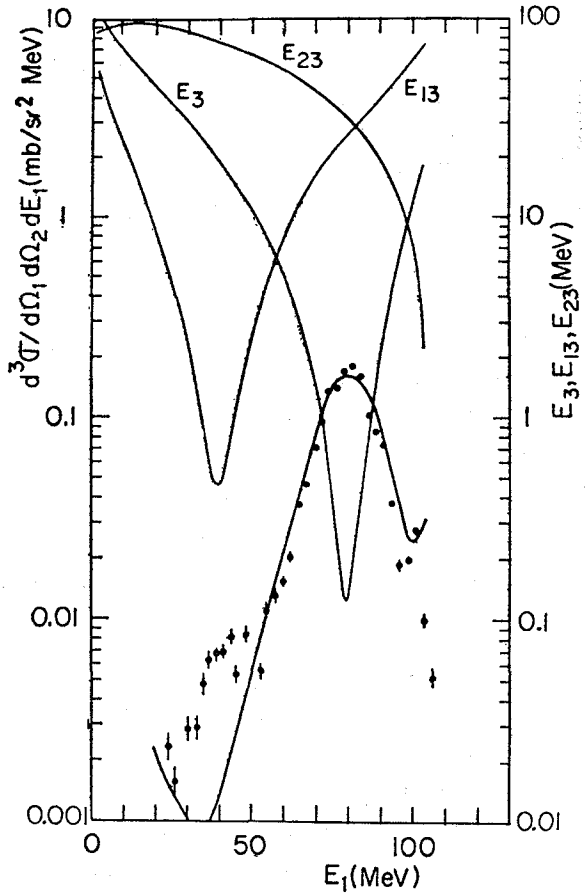

Fig. 14–5. The $d^3\sigma$ spectrum for ^{3}He(p, pd)p at $\theta_d = 40°$ and $\theta_p = -70°$. Error bars indicate statistical errors. The solid curve E_{13} and E_{23} correspond, respectively, to the relative energy of the spectator proton and a deuteron entering into the first telescope and that of the proton entering into the second telescope. The solid line along the experimental points is the PWIA curve. From [75–3].

21) yield estimation of ^{10}Be, ^{53}Mn, ^{54}Mn, and so on.
22) nuclei far from the beta stable line.
23) pion induced reaction and pion chemistry.
24) (p,pπ), (p,pd), (p,pα), and so on quasi-free scattering.
25) (p,d) reaction and short range nucleon-nucleon correlation in the nucleus.
26) exsistence of excited nucleons in the nucleus.
27) pion production from the nucleus.
28) high spin state of the nucleus induced by (p,π) reaction.
29) tertiary fission of the nucleus.

and so on.

Instrumentation items discussed were:

1) slow extraction system of the 500 MeV protons from the booster synchrotron.
2) design study of achromatic-monochromatic beam transport system.
3) design study of polarized ion source.
4) design study of oriented nuclear targets.
5) design study of radiation shielding.
6) design study of irradiation system and laboratory of radiation chemistry.
7) design study of correlated spectrometer.
8) design study of wide angle, high resolution spectrograph.
9) instrumentations for health physics.
10) application method of hydrogen bubble chamber to nuclear experiments.
11) design study of beam channel components.
12) design study of the arrangement of experimental areas.

and so on.

As a result of these efforts, the interest of the Japanese physicists and chemists in the intermediate energy nuclear physics was very much excited and proposals to the National Laboratory were made by many researchers.

XV. PUBLICATIONS

In this section, the papers published in the period from 1966 to 1976 are listed. In compilation, following criteria are adoped.

1) Scientific articles written by members of the laboratory.
2) Scientific articles of works done by using the Kyoto University Cyclotron.
3) Review articles written or edited by members of this laboratory.

Results are listed in the following table. In the table, first column indicates reference numbers in this report, second column names of authors, third column the titles of articles and the fourth column the names of journals in which the articles were published.

Table XV–1. List of Publications

Ref. No.	Author	Title	Journal
66–1	I. KUMABE, H. OGATA, S. TOMITA, M. INOUE, Y. OHKUMA.	Elastic and Inelastic Scattering of 28.4 MeV Alpha Particles by Sn, Cd, Ag, and Ti.	*J. Phys. Soc. Japan*, **21**, 413 (1966).
66–2	J. KOKAME, K. FUKUNAGA, H. NAKAMURA.	On the 3^- State in ^{28}Si and ^{24}Mg.	*Physics Letters*, **20**, 672 (1966).
66–3	K. OTOZAI, S. KUME, M. KOYAMA, T. MITSUI, T. NISHI, I. FUJIWARA.	Excitation Functions for the Reactions Induced by Deuterons on ^{142}Ce up to 14.2 MeV.	*Nucl. Physics*, **81**, 322 (1966).
66–4	K. OGINO, S. MAEDA.	The Measurement of Nuclear Reaction Cross Section at 180°.	*Genshikaku-Kenkyu*, **11** 279 (1966).

Table XV–1. List of Publications (continued)

Ref. No.	Author	Title	Journal
66–5	J. KOKAME.	A Program of a Computer (KDC-1) for Automatic Data Process of Pulse Height Spectra in Experimental Nuclear Physics.	*Bull. Inst. Chem. Res. Kyoto Univ.*, **44**, 367 (1966).
66–6	D. C. NGUYEN.	Elastic and Inelastic Scattering of Deuterons from Be^9, C^{12}, N^{14}, and O^{16} at 14 MeV.	*J. Phys. Soc. Japan*, **21**, 2462 (1966).
66–7	T. H. KIM.	Two Particle States Excited by the (α, d) Reactions on s-d Shell Nuclei.	*ibid.*, **21**, 2445 (1966).
67–1	K. FUKUNAGA, H. NAKAMURA, T. TANABE, K. HOSONO, S. MATSUKI.	Continuous Energy Spectra of Protons and Alpha Particles Emitted by the Deuteron and Alpha Particle Reaction.	*ibid.*, **22**, 28 (1967).
67–2	K. FUKE, S. KAWASAKI, T. YAMAKAWA, S. YAMAGUCHI, K. FUKUNAGA, J. KOKAME, S. YAMASHITA, T. YANABU.	Electron Beam Extraction from INS AG Synchrotron. Part II. Experiment.	*Japanese J. Appl. Phys.*, **6**, 242 (1967).
67–3	K. TAKIMOTO.	$(p, p\alpha)$ and $(\alpha, 2\alpha)$ Reactions at Medium Energy and Alpha-Clustering Correlations in Light Nuclei.	*Memoirs Coll. Sci. Univ. of Kyoto, Series A*, **31**, 267 (1967).
67–4	H. NAKAMURA.	Excitation of Spin-Flip States of Light Nuclei in Inelastic Scattering of Alpha Particles.	*J. Phys. Soc. Japan*, **22**, 685 (1967).
67–5	I. KUMABE, H. OGATA, T. H. KIM, M. INOUE, Y. OHKUMA.	Energy Spectra of Inelastic Scattering of 28.4 MeV Alpha Particles.	*ibid.*, **23**, 147 (1967).
67–6	K. FUKUNAGA, H. NAKAMURA, N. FUJIWARA.	Inelastic Scattering of Alpha Particles by Be^9 at 28.5 MeV.	*ibid.*, **23**, 911 (1967).
67–7	T. SIDEI, J. MUTO, I. KUMABE, H. OGATA, K. TAKIMOTO, Y. OHKUMA, H. INOUE Y. OGATA, Y. UEMURA, S. YAMASHITA, G. IMAMURA, T. TAKAGI, Y. YOKOTA, K. INOUE, T. TAKABE, T. OHAMA.	Kyoto University Tandem Van de Graaff.	*Memoirs Coll. Sci. Univ. of Kyoto, Series of Physics, Astrophysics, Geophysics and Chemistry*, **32**, 1 (1967).
67–8	H. ITOH.	The Elastic Scattering of 14.2 MeV Deuterons by Deuterons and Helium 4 Nuclei.	*ibid.*, **32**, 37 (1967).
67–9	K. FUKUNAGA, T. TANABE, S. YAMASHITA, N. FUJIWARA, S. KAKIGI, T. YANABU.	Breakup of Deuterons by Alpha Particle Impact.	*Contributions to Int. Conf. on Nuclear Structure Tokyo Japan*, p. 39 (1967).

Table XV–1. List of Publications (continued)

Ref. No.	Author	Title	Journal
67–10	S. YAMASHITA, S. MATSUKI, K. FUKUNAGA, D. C. NGUYEN, N. FUJIWARA, T. YANABU.	The Structure of Li^6 and Li^7 in Excited States.	*ibid.*, p. 253.
67–11	T. YANABU, S. YAMASHITA, S. KAKIGI, D. C. NGUYEN, N. FUJIWARA, K. HOSONO, S. MATSUKI, T. TANABE, K. TAKIMOTO, K. OGINO, R. ISHIWARI.	Quasi-Free Proton-Alpha and Alpha-Alpha Collisions in Be^9 and Other Light Nuclei.	*ibid.*, p. 261.
67–12	S. KAKIGI, K. HOSONO, H. NAKAMURA, D. C. NGUYEN, N. FUJIWARA, T. YANABU.	Core Excitation of Light Odd Nuclei by (d,p) Reaction.	*ibid.*, p. 276.
67–13	N. IMANISHI, F. FUKUZAWA, M. SAKISAKA, Y. UEMURA.	Coulomb Excitation of ^{45}Sc, ^{75}As, ^{127}I and ^{133}Cs.	*Nucl. Physics*, **A101**, 654 (1967).
67–14	F. FUKUZAWA, N. IMANISHI, M. SAKISAKA, K. YOSHIDA, Y. UEMURA, S. KAKIGI, H. FUJITA.	Subharmonic Acceleration of Heavy Ions by the Cyclotron of Kyoto University.	*Bull. Inst. Chem. Res., Kyoto Univ.*, **45**, 363 (1967).
67–15	R. ISHIWARI, N. SHIOMI, Y. MORI, T. OHATA, Y. UEMURA.	Comparison of Energy Losses of Protons and Deuterons of Exactly the Same Velocity.	*ibid.*, **45**, 379 (1967).
68–1	T. YANABU, S. YAMASHITA, K. HOSONO, S. MATSUKI, T. TANABE, K. TAKIMOTO, Y. OHKUMA, K. OGINO, S. OKUMURA, R. ISHIWARI.	Quasi-Free α-α Scattering in Be^9 and C^{12} at 37 MeV.	*J. Phys. Soc. Japan*, **24**, 667 (1968).
68–2	K. OTOZAI, S. KUME, H. OKAMURA, A. MITO, T. NISHI, I. FUJIWARA.	Excitation Functions for Deuteron-Induced Reactions.	*Nucl. Physics*, **A107**, 427 (1968).
68–3	S. MATSUKI.	Disintegration of Li^7 and Li^6 by 29.4 MeV Alpha-Particles.	*J. Phys. Soc. Japan*, **24**, 1203 (1968).
68–4	T. TANABE.	Breakup of Deuterons by Impact of Alpha Particle and Deuteron.	*ibid.*, **25**, 21 (1968).
68–5	K. HOSONO.	j-Forbidden (d, p) Stripping Reactions on C^{12}, O^{16}, and Mg^{24}.	*ibid.*, **25**, 36 (1968).
68–6	N. FUJIWARA.	Experimental Techniques of the 1 GeV Proton-Nucleus Reaction Experiments.	*Genshikaku-Kenkyu*, **13**, 234 (1968).
68–7	K. FUKE, Y. KOBAYASHI, T. YAMAKAWA, S. YAMAGUCHI, S. YAMASHITA,	One-Third Resonance Extraction from INS AG Electron Synchrotron.	*Japanese J. Appl. Phys.*, **7**, 1274 (1968).
68–8	I. KUMABE, M. MATOBA, E. TAKASAKI.	Inelastic Alpha-Particle Scattering on Copper 65 at 29 MeV.	*J. Phys. Soc. Japan*, **25**, 301 (1968).

Table XV–1. List of Publications (continued)

Ref. No.	Author	Title	Journal
68–9	S. KAKIGI, N. FUJIWARA, K. FUKUNAGA, D. C. NGUYEN, S. YAMASHITA, T. YANABU.	$B^{11}(\alpha, Li^7)Be^8$ Reaction at 28.4 and 29.0 MeV.	*J. Phys. Soc. Japan*, **25**, 1214 (1968).
68–10	M. MATOBA.	(α, t) Reaction on Medium-Weight Odd-Mass Nuclei. (1) ^{51}V and ^{55}Mn.	*Nucl. Physics*, **A118**, 207 (1968).
68–11	H. ITOH.	Phenomenological Potential for d-d Elastic Scattering.	*Prog. Theor. Phys.*, **39**, 1361 (1968).
69–1	S. YAMASHITA, S. KAKIGI, N. FUJIWARA, D. C. NGUYEN, K. HOSONO, S. MATSUKI, T. TANABE, T. YANABU, K. TAKIMOTO, K. OGINO, R. ISHIWARI.	Quasi-Free Scattering in the Reaction $Be^9(p, p\alpha)He^5$ at 55 MeV.	*J. Phys. Soc. Japan*, **26**, 1078 (1969).
69–2	S. MATSUKI, S. YAMASHITA, K. FUKUNAGA, D. C. NGUYEN, N. FUJIWARA, T. YANABU.	Elastic and Inelastic Scattering of 14.7 MeV Deuterons and of 29.4 MeV Alpha-Particles by Li^6 and Li^7.	*ibid.*, **26**, 1344 (1969).
69–3	S. MATSUKI.	$Li^7(\alpha, t)\alpha\alpha$ Reaction.	*Soryushiron Kenkyu*, **39**, 303 (1969).
69–4	N. FUJIWARA.	Three Body Reaction of Light Nuclei.	*ibid.*, **39**, 305 (1969).
69–5	K. KOMURA, T. MITSUGASHIRA, A. MITO, K. OTOZAI.	Target Chemistry of Ruthenium.	*Bull. Inst. Chem. Res. Kyoto Univ.*, **47**, 79 (1969).
69–6	K. FUKUNAGA, S. MATSUKI, N. FUJIWARA, T. MIYANAGA.	Transistorized Circuits for the Fast Coincidence Experiments.	*ibid.*, **47**, 83 (1969).
69–7	Y. UEMURA, J. KOKAME, S. YAMASHITA, S. KAKIGI, H. FUJITA, S. KAKUI, T. MARUYAMA, K. SANO, F. FUKUZAWA.	The Ion Source for the Cyclotron of Kyoto University.	*ibid.*, **47**, 97 (1969).
69–8	Y. UEMURA, S. KAKIGI, N. FUJIWARA, S. MATSUKI, H. NAKAMURA, T. H. KIM, K. OGINO, N. IMANISHI, T. KOYAMA, S. KURIYAMA,	Vacuum Evaporator with an Electron Gun for the Preparation of Thin Target.	*ibid.*, **47**, 114 (1969).
69–9	T. YANABU, K. MIYAKE, H. IKEGAMI, A. KATASE, S. YAMASHITA, T. OHAMA, K. HOSONO, S. KAKIGI, D. C. NGUYEN, R. ISHIWARI.	Beam Transport System of the Kyoto University Cyclotron.	*ibid.*, **47**, 123 (1969).
69–10	Y. UEMURA, S. YAMASHITA, T. YANABU, Y. YAMADA.	Design and Performance of a Broad Range Magnetic	*ibid.*, **47**, 143 (1969).

Table XV–1. List of Publications (continued)

Ref. No.	Author	Title	Journal
	T. OHAMA, S. KAKIGI, D. C. NGUYEN.	Spectrograph.	
69–11	T. YANABU, H. FUJITA, M. GOTOH, T. IWASA,	A Scattering Chamber for Three Body Nuclear Reactions.	*ibid.*, **47**, 154 (1969).
69–12	T. NISHI, K. OTOZAI.	Excitation Functions of Deuteron Induced Reactions.	*ibid.*, **47**, 162 (1969).
69–13	A. MITO, K. KOMURA, T. MITSUGASHIRA, K. OTOZAI.	Excitation Functions for the (d, p) Reactions on ^{96}Ru, ^{102}Ru, and ^{104}Ru.	*Nucl. Physics*, **A129**, 165. (1969)
69–14	T. YANABU.	Nuclear Relaxation and Its Analogy in Properties of Bulk Material.	*JAERI*, **No. 1184** p. 131 (1969).
69–15	T. YANABU.	A Review of the Intermediate Energy Nuclear Physics Research in Japan.	*Design Study Report of the Laboratory of Elementary Particles*, p. 175 (1969).
69–16	N. FUJIWARA.	$B^{11}+\alpha\rightarrow\alpha+\alpha+Li^7$ Reaction at 28.5 MeV.	*J. Phys. Soc. Japan*, **27**, 1380 (1969).
70–1	N. FUJIWARA.	The (p, pd) Reaction as a Tool to Investigate the Nucleon-Nucleon Short Range Correlation in the Nucleus.	*Genshikaku-Kenkyu*, **15**, 55 (1970).
70–2	M. YASUE, N. FUJIWARA, T. OHSAWA, N. IZUTSU.	Heavy Particle Identification with a T. O. F. Method in Nuclear Reactions.	*Bull. Inst. Chem. Res., Kyoto Univ.*, **48**, 223 (1970).
70–3	K. HOSONO, S. KAKIGI, H. NAKAMURA, N. FUJIWARA, D. C. NGUYEN, T. YANABU.	Broad Energy Protons from the Reaction $C^{12}+d\rightarrow p+C^{13}$ (7.64 MeV and 8.33 MeV).	*ibid.*, **48**, 269 (1970).
70–4	T. YANABU editor	Report on the Meeting of Intermediate Energy Nuclear Physics in Japan	*Genshikaku-Kenkyu*, **14**, 827 (1970).
70–5	T. YANABU, R. TAMAGAKI, Y. YASUNO, H. HISATAKE editors	Report on the Workshop of Nuclear Physics in the National Institute for High Energy Physics.	*ibid.*, **15**, 3 (1970).
71–1	R. ISHIWARI, N. SHIOMI, S. SHIRAI, T. OHATA, Y. UEMURA.	Comparison of Stopping Powers of Al, Ni, Cu, Rh, Ag, Pt, and Au for Protons and Deuterons of Exactly the Same Velocity.	*Bull., Inst. Chem. Res. Kyoto Univ.*, **49**, 390 (1971).
71–2	R. ISHIWARI, N. SHIOMI, S. SHIRAI, T. OHATA, Y. UEMURA.	Stopping Powers of Be, Al, Cu, Mo, Ta, and Au for 28 MeV Alpha Particles.	*ibid.*, **49**, 403 (1971).
72–1	M. YASUE, T. OHSAWA, N. FUJIWARA, S. KAKIGI, D. C. NGUYEN, S. YAMASHITA.	Excited States of ^{10}B near 10 MeV Studied by Proton Induced Reactions on ^{9}Be.	*J. Phys. Soc. Japan*, **33**, 265 (1972).

Table XV–1. List of Publications (continued)

Ref. No.	Author	Title	Journal
72–2	S. MATSUKI, M. YASUE, K. TSUJI, N. IZUTSU, S. YAMASHITA.	The D(p, 2p)n Reaction at 3.8 to 5.0 MeV.	*Proc. Int. Conf. on Few Particle Problems in the Nuclear Interaction Los Angeles,* Sept. 1972 p. 535.
72–3	S. YAMASHITA, S. KAKIGI, N. FUJIWARA, T. OHSAWA, K. TAKIMOTO, K. OGINO, I. YAMANE, M. YASUE, N. IZUTSU, D. C. NGUYEN.	Three Body Breakup of ^{12}C by 52 MeV Protons.	*ibid.,* p. 1007.
72–4	M. YASUE, T. OHSAWA, N. FUJIWARA, S. KAKIGI, D. C. NGUYEN.	Structure of ^{10}B Formed by the Reaction $^{9}Be+p$.	*ibid.,* p. 1009.
72–5	S. HIRAMATSU, T. KAMAE, H. MURAMATSU, K. NAKAMURA, N. IZUTSU, Y. WATASE.	(e, e′p) Reactions on $^{6,7}Li$, ^{9}Be, ^{12}C, ^{27}Al, ^{40}Ca, and ^{51}V.	*Proc. Int. Conf. on Nuclear Structure Studies Using Electron Scattering and Photoreaction,* Sendai. Sept. 1972 p. 429 (1972).
73–1	N. FUJIWARA, T. OHSAWA, S. TANAKA, T. YANABU.	Particle Production in Interaction of 8 GeV Protons with Nuclei.	*Genshikaku-Kenkyu,* **18**, 282 (1973).
73–2	S. HIRAMATSU, T. KAMAE, H. MURAMATSU K. NAKAMURA, N. IZUTSU, Y. WATASE.	Quasi-Free Electron Scattering on Light Nuclei.	*Physics Letters,* **44B**, 50 (1973).
74–1	T. YANABU editor	Design Studies on Nuclear Experiment Facilities Coupled with the Booster Beam of the National Laboratory for High Energy Physics.	*Genshikaku-Kenkyu,* **18**, 381 (1974).
74–2	M. YASUE.	Energy Dependence of the Reaction $^{9}Be(p, p_1)^{9}Be^*$ (1.67).	*J. Phys. Soc. Japan,* **36**, 1254 (1974).
74–3	R. ISHIWARI, N. SHIOMI, S. SHIRAI, Y. UEMURA.	Stopping Powers of Al, Ti, Fe, Cu, Mo, Ag, Sn, Ta, and Au for 7.2 MeV Protons.	*Bull. Inst. Chem. Res. Kyoto Univ.,* **52**, 19 (1974).
74–4	N. FUJIWARA, T. OHSAWA, T. MIYANAGA, K. FUKUNAGA, S. KAKIGI.	Some Experiments on the Radio-frequency System of the Improved University Cyclotron.	*ibid.,* **52**, 70 (1974).
74–5	Y. UEMURA, K. FUKUNAGA, S. KAKIGI, T. YANABU, N. FUJIWARA, T. OHSAWA, H. FUJITA, T. MIYANAGA, D. C. NGUYEN,	Improved Kyoto University Cyclotron.	*ibid.,* **52**, 87 (1974).

Table XV–1. List of Publications (continued)

Ref. No.	Author	Title	Journal
74–6	Y. UEMURA, T. NISHI, N. IMANISHI, I. FUJIWARA.	Residual Radioactivity of the Kyoto University Cyclotron.	*ibid.*, **52**, 124 (1974).
74–7	M. YASUE, T. OHSAWA, N. FUJIWARA, S. KAKIGI, D. C. NGUYEN, S. YAMASHITA.	Proton Induced Reactions on ^{9}Be from 4 to 6 MeV.	*ibid.*, **52**, 177 (1974).
74–8	S. MATSUKI, S. YAMASHITA, N. FUJIWARA, K. FUKUNAGA, D. C. NGUYEN, T. YANABU.	The ^{7}Li(α, t)$\alpha\alpha$ and ^{6}Li(α, d)$\alpha\alpha$ Reactions at 29.4 MeV.	*ibid.*, **52**, 202 (1974).
74–9	S. KAKIGI, N. FUJIWARA, K. FUKUNAGA, T. OHSAWA, D. C. NGUYEN, T. YANABU, M. YASUE, S. YAMASHITA.	^{11}B(p, α)^{8}Be(α)^{4}He Reaction at 7.3 MeV.	*ibid.*, **52**, 218 (1974).
74–10	J. KOKAME,	Optical Model Parameters of Several s-d Shell Nuclei for 28 MeV alpha-Particle Scattering.	*ibid.*, **52**, 227 (1974).
74–11	T. NISHI, I. FUJIWARA, N. IMANISHI, H. NAKAMURA, H. OKAMOTO.	Excitation Functions for the Deuteron Induced Reactions on ^{64}Zn and ^{76}Ge.	*ibid.*, **52**, 233 (1974).
74–12	R. FRASCARIA, P. G. ROOS, M. MORLET, N. MARTY, V. COMPARAT, N. FUJIWARA, A. WILLIS.	Quasi Free pp and pd Scattering on ^{4}He at 155 MeV.	*Contributions to the Int. Conf. of Few Body Problems in Nuclear and Particle Physics, Quebec, Canada,* August, 1974 p. 107.
74–13	J. P. DIDELEZ, R. FRASCARIA, N. FUJIWARA, I. D. GOLDMAN, E. HOURANY, H. NAKAMURA-YOKOTA, F. REIDE, T. YUASA,	Proton Indused ^{3}He Break-up at 156 MeV.	*ibid.*, p. 110.
74–14	T. YANABU, N. FUJIWARA, T. OHSAWA, S. TANAKA.	Pion and Deuteron Production from the Nucleus at High Energies.	*Genshikaku-Kenkyu*, **19**, 553 (1974).
74–15	R. ISHIWARI, N. SHIOMI, S. SHIRAI, Y. UEMURA.	Stopping Powers of Al, Ti, Fe, Cu, Mo, Ag, Sn, Ta, and Au for 7.2 MeV Protons.	*Physics Letters*, **48A**, 96 (1974).
74–16	K. NAKAMURA, S. HIRAMATSU, T. KAMAE, H. MURAMATSU, N. IZUTSU, Y. WATASE.	Reaction ^{40}Ca(e, e′p) and Observation of the 1s Proton State.	*Phys. Rev. Letters*, **33**, 853 (1974).
75–1	R. FRASCARIA, P. G. ROOS, M. MORLET, N. MARTY, A. WILLIS, V. COMPARAT, N. FUJIWARA.	^{4}He(p, 2p)^{3}H and ^{4}He(p, pd)^{2}H Reaction at 156 MeV.	*Phys. Rev. C*, **12**, 243 (1975).
75–2	V. COMPARAT, R. FRASCARIA, N. FUJIWARA, N. MARTY, M. MORLET, P. G. ROOS, A. WILLIS.	Elastic Proton Scattering on ^{4}He at 156 MeV.	*ibid.*, **12**, 251 (1975).

Table XV-1. List of Publications (continued)

Ref. No.	Author	Title	Journal
75–3	J. P. DIDELEZ, R. FRASCARIA, N. FUJIWARA, I. D. GOLDMAN, E. HOURANY, H. NAKAMURA-YOKOTA, F. REIDE, T. YUASA.	Proton Induced ^{3}He Break-up at 156 MeV.	*Phys. Rev. C*, **12**, 1974 (1975).
76–1	T. MIYANAGA, T. OHSAWA, S. TANAKA, N. FUJIWARA, S. KAKIGI, K. FUKUNAGA, T. YANABU.	Multiparameter Data Acquisition System with a Mini-Computer.	*Bull. Inst. Chem. Res. Kyoto Univ.*, **54**, 1 (1976).
76–2	T. TANABE, K. KOYAMA, M. YASUE, H. YOKOMIZO, K. SATO, J. KOKAME, N. KOORI, S. TANAKA,	The (^{3}He, ^{3}He), (^{3}He, ^{3}He′) and (^{3}He, α) Reactions on ^{12}C at 82.1 MeV.	*J. Phys. Soc. Japan*, **41**, 361 (1976).
76–3	K. NAKAMURA, N. IZUTSU.	On the Final State Interactions in (e, e′p) Reactions.	*Nucl. Physics*, **A259**, 301 (1976).

In conclusion, the cyclotron in our laboratory worked well in this decade, and was used by many researchers in many fields of research. The improvement was successful and the cyclotron recovered its usefulness. Many items were continuously investigated and characteristics of the Kyoto Cyclotron Laboratory was established. However, the inflation and the appearance of new type accelerators lessened the feasibility of the conventional cyclotron in our laboratory. Therefore, a new stage of investigations with new accelerators are necessary and is hoped by many researchers of the Kyoto University.

ACKNOWLEDGMENTS

This article is dedicated to the late Professor Y. Uemura. We are much obliged to him for his self sacrificing life and continual efforts to maintain the activities of the Laboratory of Nuclear Science. Now, the author would like to acknowledge the authorities of the Kyoto University and of the Ministry of Education for their financial support of the cyclotron improvement. Also we would like to thank the past Directors of the Institute for Chemical Research, Professor Sango Kunichika, Professor Waichiro Tsuji, Professor Eiji Suito, and Professor Yoshimasa Takezaki, and the present Director of the Institute, Professor Tsunenobu Shigematsu, for their kind arrangements and encouragements. Thanks are also due to Professor K. Kimura, Professor M. Sonoda, Professor S. Shimizu, Professor R. Ishiwari, Professor J. Kokame, Professor A. Katase, Professor I. Kumabe, Professor S. Yamashita, Professor H. Takekoshi, Professor K. Miyake, and Professor H. Ikegami for the foundation of the Laboratory. We are much obliged also to the Mitsubishi Heavy Industries Ltd., Fuji Electronic Industrial Co., Shimazu Seisakusho Ltd., Japan Panel Service Inc., and Origin Electric Co., for their patient cooperation to re-new the cyclotron. Many researchers who cooperate with the Laboratory and achieved important investigations are appreciated. Among these researchers, Professor T. Nishi and his collaborators are especially acknowledged for their kind cooperation and inspiring advices.